Multi-threaded real root isolation on multi-core architectures

(Spine title: Real Root Isolation for Polynomial System Solvers)

(Thesis format: Monograph)

by

A.B.M. Zunaid Haque

Graduate Program
in
Computer Science

A thesis submitted in partial fulfillment
of the requirements for the degree of
Master of Science

The School of Graduate and Postdoctoral Studies
The University of Western Ontario
London, Ontario, Canada

Abstract

Today, most computer algebra systems offer efficient solvers for computing the complex solutions of polynomial systems with rational number coefficients. However, very limited support is available for calculating their real solutions, in particular when there are infinitely many such solutions. Various factors (mathematical and computational difficulties) explain this situation. To address this challenge, high-performance implementation targeting clusters of multicore and manycore processors is a necessity.

Isolating the real roots of univariate polynomials is at the core of the algorithms computing exactly the real solutions of polynomial systems. Applications of such tools spread in robotics, program verification, dynamical system analysis, etc.

In this report, we first review the principles and implementation techniques of real root isolation algorithms based on the so-called Descartes' rule of signs. This technique provides opportunities to design optimized parallel and cache-friendly algorithms, well suited for multicore architectures. However, state-of-the-art implementations exhibit satisfactory performances regarding parallelism only for input polynomials of very large degrees, say in the order of thousands.

In this proposal, we investigate ideas to overcome this limitation. We observe that, due to expression swell, arithmetic operations on the coefficients provide additional opportunities for parallelism, To exploit this observation, we consider two techniques. One is based on parallel prefix-sum computations. The other one uses a blocking strategy with dynamic block size.

Keywords. Real root isolation, taylor-shift, prefix-sum, blocking, Parallelism, Muticore architectures.

Contents

List of Algorithms

List of Figures

List of Tables

Chapter 1

Introduction

Today, most computer algebra systems offer efficient solvers for computing the complex solutions of polynomial systems. Some of them, such as Maple, provide tools for "identifying" which of those solutions are real, provided that the input system has finitely many solutions. The case of systems with infinitely many real solutions has very limited support. This severely limits the impact of computer algebra in the areas which are in need of exact calculation with real numbers, such as robotics, program verification, dynamical system analysis.

In "Triangular decomposition of semi-algebraic systems", C. Chen, J. H. Davenport, J. P. May, M. Moreno Maza, B. Xia and R. Xiao [4] propose an algorithm for solving any system of polynomial equations, inequations and inequalities. Under genericity assumption, this algorithm runs in singly exponential time with respect to the number of variables improving on previously established methods. Their implementation in Maple, shows promising results. However, this type of algorithm is highly demanding in computing resources, which restricts the range of the problems that an implementation can solve on traditional personal computers. To address this challenge, our research group is developing a high-performance implementation targeting clusters of multicores.

This thesis work contributes to this project by investigating and deploying parallel algorithms for isolating the real roots of univariate equations with rational number coefficients. This type of calculation is at the core of the computation of the real solutions of polynomial systems and efficient sequential algorithms are available for this task [18, 19].

We devote our effort to the parallelization of an algorithm, called the Vincent-Collins-Akritas (VCA) Algorithm [7, 21], for isolating (that is, identifying) the real roots of a univariate polynomial with rational number coefficients. As analyzed by

many researchers [5, 8] the parallelization of the VCA Algorithm reduces to the parallel calculation of the *Taylor shift by 1 of a polynomial*. Although there exist asymptotically fast algorithms (running essentially in linear time with respect to the size of the input) for this task, these are not suitable for multicore architectures due to the fine-grained parallelism that these fast algorithms require. In fact, the only practical parallel algorithmic solutions for Taylor shift computation on multicore architectures are based on the construction of the Pascal Triangle.

This latter problem, and more generally the problems of parallel tableau constructions, parallel stencil computations are well known challenges in parallel processing [12]. One of the challenge is the *low parallelism* of these algorithms. More precisely, for an input polynomial of degree n, in the fork-join parallelism model [11], the best known complexity estimates for the parallel construction of the Pascal Triangle are obtained via a blocking strategy. If the block order is B, the work is in $\Theta(n^2)$ and the parallelism is in $\Theta(n/B)$. Moreover, for an ideal cache of Z words and cache lines of L words, the cache complexity (of the serial counterpart of this algorithmi) is in $\Theta(n^2/(ZL))$, provided that B is well chosen. Therefore, one can say that the parallelism is sub-linear, which is generally too low for multicore implementation. Another scheme for the parallel construction of the Pascal Triangle is based on a divide and conquer approach which has similar cache complexity and has the advantage to be cache oblivious. However its parallelism is even less than that of the blocking strategy.

Section 2 provides background materials on both real root isolation and multicore programming. Sections 3 and 4 review respectively the blocking strategy and divide and conquer approaches for Taylor shift computations.

Our objective in this thesis is to increase to performances of real root isolation on multicore architectures in terms of parallelism and cache complexity. By increasing the performances of this operation, we expect to tackle harder problems on available parallel architectures. In fact, this idea has actually been successfully initiated in [5]. Moreover, the parallelization challenges posed by real root isolation algorithms are typical from symbolic computation. Thus, the solutions developed in this thesis research could benefit to other subjects in this area.

The contributions of this thesis are three-fold.

In Chapter 5, we observe that the fork-join parallelism model does not apply to parallel Taylor shift computation for polynomials of sufficiently large degrees. This is because the fork-join parallelism model assumes that each strand works in unit in time while the growth of the intermediate coefficients in the Pascal Triangle computation

invalidates this assumption. Therefore, we provide a more realistic analysis of parallel Taylor shift computation for polynomials of large degrees. This analysis shows that the parallelism is in fact higher than in the naive analysis, but only by a constant factor. This analysis also shows that the burdened span grows asymptotically faster than the non-burdened span, which was a great surprise to us and which can be seen as an additional challenge for the parallelization of real root isolation on multicore architectures.

In Chapter 6, we explore the divide and conquer scheme. Based on the study conducted in Section 5, due the growth of the intermediate coefficients in the Pascal Triangle construction, we observe that two recursive calls in that scheme are likely to have different work load and different amount of cache misses. We propose different solutions to cope with this problem and our experimentation illustrates their benefits.

In Chapter 7, we explore the blocking strategy. Based on the study conducted in Section 5, we turn the original blocking strategy described in [6] into a poly-algorithm which can adapt the granularity of its parallelism depending on the local size of the data. Experimentation illustrates the effectiveness of this approach.

Chapter 2

Background

This chapter presents background materials which are used throughout this thesis. Section 2.1 is a brief introduction on techniques for finding the real roots of univariate polynomials. Descartes' famous rule of signs is discussed in Section 2.2. Section 2.3 is a review of Collin-Akritas Algorithm (VCA) for real root isolation. In Section 2.5, the Taylor Shift operation, which is the core routine for VCA, is discussed together with Horner's Method and Pascal's Triangle construction. Recall that this thesis focuses on the parallelization of Taylor Shift computations targeting multicore architectures. Other techniques could be considered for the parallelization of the VCA Algorithm and we will leave that for future works.

This chapter contains also a review of various aspects of multithreaded programming on multicore architectures. A brief discussion on cache memories and cache complexity is given in Section 2.6. Section 2.7 is a review on multicores as our implementation is based on this architecture. Finally Section 2.8 is a brief overview of the fork-join parallelism model and *Cilk++*. For these materials on programming and architectures we follow the lecture notes of the UWO courses CS9624-4435 and CS5635-4402 which can be found at `http://www.csd.uwo.ca/~moreno/CS9624-4435-1011.html` and at `http://www.csd.uwo.ca/~moreno/CS9535-4402-1112.html`, respectively.

2.1 Real root isolation

Given a univariate polynomial f, a root finding algorithm is a numerical method for computing a value x_0 for which $f(x_0) = 0$ holds. Such an x_0 is called a *root* of the polynomial f. An important observation is that, even if the coefficients of f are numerical, one may not be able to represent x_0 exactly as a floating point number. For instance if $f(x) = x^2 - 2$ then f has two real roots $\sqrt{2}$ and $-\sqrt{2}$, none of them

being a rational number. However, for each real root x_0 of f it is always possible to find an interval $[s_0, t_0]$ with rational end points such that $[s_0, t_0]$ contains x_0 and does not contain any other real roots of f. Determining such an interval $[s_0, t_0]$ for each real root x_0 of f is referred as *isolating the real roots of* f. This leads to the following definition.

Definition 1. *Let* $f \in \mathbb{R}[x]$ *be a non-constant polynomial. We say that pairwise disjoint intervals* $[s_0, t_0], [s_1, t_1], \ldots, [s_e, t_e]$ *with rational end points* isolate the real roots *of* f *(or form a* real root isolation *of* f*) if*

1. *any real root of* f *is contained in one of the intervals* $[s_0, t_0], \ldots, [s_e, t_e]$,
2. *each of these intervals contains exactly one real root of* f.

Sturm's Theorem and Descartes' rule of signs [2] are building blocks for finding the real roots location or separating them. Several algorithms are well-known, such as Vincent-Collins-Akritas Algorithm [7, 21], Krandick's Algorithm [17]. Based on those, several more recent and more sophisticated algorithms have been introduced; they improve certain aspects such as arithmetic complexity or memory usage. In their paper "Efficient isolation of polynomial real roots" [18], Fabrice Rouillier and Paul Zimmermann discuss memory consumption of sequential algorithms for real root isolation. These considerations, however, do not apply to our context of multithreaded programming targeting multicores. Indeed, in a parallel setting, real root isolation leads to concurrent Taylor shift computations, thus to unavoidable data duplication, which is what the Authors of [18] try to avoid. In the context of multicores, the main memory issue that we want to address is to minimize cache complexity, which is not the scope of [18].

2.2 Descartes' rule of signs

Using Descartes' rule of signs we can derive a bound on the number of positive real roots of a polynomial. Before stating Descartes' rule of signs as Theorem 1, we specify in Definition 2, how to count the number of sign changes in a sequence of real numbers.

Definition 2. *Let* $a_0, a_1, \ldots, a_n$ *be a sequence of* $(n+1)$ *real numbers. For* i, j *in the interval* $[0, \ldots, n]$*, with* $i < j$*, we say that there is a* sign change from a_i to a_j *if the following two conditions hold*

(*i*) $a_i a_j < 0$ *holds and,*

(*ii*) *for all* k *with* $i < k < j$ *we have* $a_k = 0$.

Theorem 1. *Let $f \in \mathbb{R}[x]$ be a polynomial with real coefficients $a_n, a_{n-1}, \ldots, a_0$, written as:*

$$f = a_n\, x^n + a_{n-1}\, x^{n-1} + \cdots + a_0$$

where we assume $a_n a_0 \neq 0$. Let v be the number of sign changes in the sequence $a_n, a_{n-1}, \ldots, a_0$ and let r be the number of positive roots of f. Then, there exists a non-negative integer m such that we have $r = v - 2m$.

In particular, when $v = 0$ or $v = 1$ holds, we have $r = v$. That means that, when the number of sign change is 0 or 1, we know that the number of positive real roots is 0 or 1, respectively.

2.3 Vincent-Collins-Akritas Algorithm

Let $p \in \mathbb{Q}[x]$ be a non-constant polynomial with rational number coefficients and let $]a, b[$ be an (non-empty) open interval of $\mathbb{Q}$. In this section, we present an algorithm for isolating the real roots of p, as specified in Definition 1.

This algorithm, based on the ideas of Vincent [21] and more recently the work of Collins and Akritas [7] relies on Descartes' rule of signs. More precisely, this algorithm uses Descartes' rule to obtain an upper bound for the number of real roots of p in $]a, b[$. To justify this algorithm, we consider the following two polynomial functions:

$$f_1 : \left\{ \begin{array}{ccc}]a,b[& \to & \mathbb{R} \\ x & \longmapsto & p(x) \end{array} \right. \quad \text{and} \quad f_2 : \left\{ \begin{array}{ccc}]0,\infty[& \to & \mathbb{R} \\ x & \longmapsto & \overline{p}(x) \end{array} \right. \tag{2.1}$$

where $\overline{p}(x) = (x+1)^d p(u(x))$ and $u(x) = \frac{ax+b}{x+1}$. Observe that $u'(x) = \frac{a-b}{(x+1)^2}$ holds. Since we have $a - b < 0$, the function u is strictly decreasing on $]0, \infty[$. Moreover we have:

$$\lim_{x \to 0} u(x) = b \quad \text{and} \quad \lim_{x \to +\infty} u(x) = a.$$

Therefore, the function u realizes a 1-to-1 map from $]0, \infty[$ onto $]a, b[$. Next we observe that $\overline{p}(x)$ is a polynomial, thanks to the multiplication of $p(u(x))$ by $(x+1)^d$ which clears denominators out in $p(u(x))$. Now, we note the following relation, for every $x \in]0, \infty[$,

$$\overline{p}(x) = 0 \quad \Longleftrightarrow \quad p(u(x)) = 0. \tag{2.2}$$

Thus x is a positive root of the polynomial $\overline{p}$ if and only if $u(x)$ is a root of the polynomial p in $]a, b[$. Therefore, by applying Descartes' rule of signs to polynomial $\overline{p}$ we count the number of real roots of polynomial p in $]a, b[$. This proves the

correctness of Algorithm 1.

Algorithm 1: BoundNumberRootsVCA($p,]a, b[$)

Input: p squarefree polynomial $\in \mathbb{Q}[x]$ and $a \leq b$ are in $\mathbb{Q}$.
Output: Number of roots of p in the interval $]a, b[$.

1: $\overline{p} = (x+1)^d p(\frac{ax+b}{x+1})$ where d is the degree of p;
2: From $\overline{p}$ find out the coefficient sequence;
3: **return** the number of sign variations in the coefficient sequence.

Algorithm 1, in the call BoundNumberRootsVCA($p,]a, b[$), uses Descartes' rule to obtain an upper bound for the number of real roots of p in $]a, b[$. In the call RootIsolateAuxVCA($p,]a, b[$), Algorithm 2 uses Algorithm 1 to determine a real root isolation (in the sense of Definition 1) of a square free polynomial $p \in \mathbb{Q}[x]$. For the interval $]a, b[$, three cases need to be considered for the number of sign variations v,

(i) $v = 0$, thus no roots in $]a, b[$.
(ii) $v = 1$, thus a single root in $]a, b[$.
(iii) $v > 1$, in which case we cannot conclude on the number of real roots of p in $]a, b[$.

For Case (iii), the interval $]a, b[$ is divided into two equal parts and for each of them Algorithm 2 is called recursively. Also, Algorithm 2 checks whether the mid-point of the interval $m = \frac{a+b}{2}$ is itself a root or not.

Algorithm 2: RootIsolateAuxVCA($p,]a, b[$)

Input: p squarefree polynomial $\in \mathbb{Q}[x]$ and $a \leq b$ are in $\mathbb{Q}$.
Output: An interval decomposition of real roots of p in the range]a,b[.

1: v = Number of sign variations;
2: Calculate v from BoundNumberRootsVCA($p,]a, b[$);
3: **if** $v = 0$ **then**
4: | return ϕ
5: **else if** $v = 1$ **then**
6: | return]a,b[
7: **else**
8: | $m = \frac{a+b}{2}$ $res \longleftarrow \phi$;
9: | **if** $p(m) = 0$ **then**
10: | | $res \longleftarrow \{\{m\}\}$;
11: | **return** RootIsolateAuxVCA($p,]a, m[$) $\cup$ res $\cup$ RootIsolateAuxVCA($p,]m, b[$).

Algorithm 3, RootIsolateVCA(p) is the top-level procedure, which calls Algorithm 2 after determining an initial interval containing all the real roots of the input

polynomial. This initial interval can be obtained from a root bound such as the *Cauchy bound*.

Algorithm 3: RootIsolateVCA(p)

Input: p squarefree polynomial $\in \mathbb{Q}[x]$.
Output: An interval decomposition of real roots of p .
1: Calculate a strict bound H on the absolute value of any roots of p;
2: **return** RootIsolateAuxVCA($p,]-H, H[$)

To calculate the strict bound H for a polynomial $p = \sum_{i=0}^{d} c_i x^i$, there are different ways like **Cauchy bound**, which is given by $H = \frac{1}{c_d} \sum_{i=0}^{d} |c_i|$. For more details on root estimates (bounds, etc.) and for a termination proof of Algorithm 3, see the Phd Thesis of Jeremy R. Johnson [15]).

We summarize some important complexity results on the VCA Algorithm and related routines. As before, let $p \in \mathbb{Q}[x]$ be a squarefree polynomial of degree d. Let L be an upper bound of the bit size of the coefficients of p. In [20], Arnold Schönhage, with his *splitting circle method*, proved that isolating the real roots of p could be done within $O^{\sim}(Ld^3)$ bit operations. A more practical algorithm, with a slightly higher complexity of $O^{\sim}(L^2d^3)$ is proposed by Michael Sagraloff in [19]. Finally, in [9], Arno Eigenwillig, Vikram Sharma and Che K. Yap proved that the size of the recursion tree of Algorithm 5 is in $O(d(L + \log(d)))$.

2.4 A variant of the VCA Algorithm

It is not hard to see that the dominant cost in the VCA Algorithm is the computation of the polynomial

$$\overline{p} = (x+1)^d p(\frac{ax+b}{x+1}) \tag{2.3}$$

in Algorithm 1. It is, therefore, natural to dedicate one's effort on this computation. The polynomial $\overline{p}$ depends on three parameters, namely p, a, b. A first step toward optimizing this computation is to reduce the number of parameters, while maintaining (or reducing) the same algebraic complexity. There is a standard way to do this, see for instance [18] among other references. With Algorithms 4 and 5, we follow here the presentation of Changbo Chen, Marc Moreno Maza and Yuzhen Xie in their paper [5].

Clearly, the problem of isolating the real roots of p and that counting of them are essentially the same problem. Thus, one algorithm solving one of these problems can

be adapted to solve the other. Since the output of the counting problem is simpler, Algorithms 4 and 5 solve this latter problem.

Algorithm 4: realRoots(p, k)

Input: A univariate squarefree polynomial $p \in \mathbb{Q}[x]$ of degree d, an integer $k \geq 0$ such that the absolute value of any real root of p is less than or equal to 2^k.

Output: The number of real roots of p.

1: **if** $x \mid p$ **then**
2: $\quad m = 1$
3: **else**
4: $\quad m = 0$
5: $p_1 = p(2^k x)$;
6: $p_2 = p_1(-x)$;
7: $m' = \text{RootsInZeroOne}(p_1)$;
8: $m = m + \text{RootsInZeroOne}(p_2)$;
9: **return** $m + m'$.

In Algorithm 4 we transform the polynomial $p(x)$ into the polynomial $p_1(x)$ given by $p_1(x) = p(2^k x)$, so that the roots of $p(x)$ in the interval $]-2^k, 2^k[$ are 1-to-1 correspondence with the roots of $p_1(x)$ in the interval $]-1, 1[$. We can prove this fact in the following way. Let us consider two polynomial functions:

$$f_1 : \left\{ \begin{array}{ccc}]-2^k, 2^k[& \to & \mathbb{R} \\ x & \longmapsto & p(x) \end{array} \right. \quad \text{and} \quad f_2 : \left\{ \begin{array}{ccc}]0, 1[& \to & \mathbb{R} \\ x & \longmapsto & p_1(x) \end{array} \right. \tag{2.4}$$

where $p_1(x) = p(u(x))$ and $u(x) = 2^k x$. Observe that $u'(x) = 2^k$ holds, thus u is strictly increasing on $]0, 1[$. Moreover we have:

$$\lim_{x \to 0, x > 0} u(x) = 0 \quad \text{and} \quad \lim_{x \to +1, x < +1} u(x) = 2^k.$$

Therefore, the function u realizes a 1-to-1 map from $]0, 1[$ onto $]0, 2^k[$. Now, we note the following relation, for every $x \in]0, 1[$,

$$p_1(x) = 0 \quad \Longleftrightarrow \quad p(u(x)) = 0. \tag{2.5}$$

Thus, some $x \in]0, 1[$ is a root of the polynomial p_1 if and only if $u(x)$ is a root of the polynomial p in $]0, 2^k[$. Similarly, one can check that $x \in]-1, 0[$ is a root of the polynomial p_2 if and only if $u(-x)$ is a root of the polynomial p in $]-2^k, 0[$. Finally,

$x = 0$ is a root of p if and only if x divides p. Combining these three observations proves the correctness of Algorithm 4.

The main subroutine of Algorithm 4 is Algorithm 5. The most expensive operation is *Taylor shift computation*, which substitutes x to $x + 1$ in p_1 at Lines 2 and 7. Section 2.5 is dedicated to Taylor shift computation.

Algorithm 5: RootsInZeroOne(p)

Input: A univariate squarefree polynomial $p \in \mathbb{Q}[x]$ of degree d.

Output: The number of real roots of p in $(0, 1)$.

1: $p_1 = x^d p(1/x)$;
2: $p_2 = p_1(x + 1)$; /* Taylor shift */
3: Let v be the number of sign variations of the coefficients of p_2;
4: **if** $v \leq 1$ **then**
5: | return v
6: $p_1 = 2^d p(x/2)$;
7: $p_2 = p_1(x + 1)$; /* Taylor shift */
8: **if** $x \mid p_2$ **then**
9: | $m = 1$
10: **else**
11: | $m = 0$
12: $m' = \text{RootsInZeroOne}(p_1)$;
13: $m = m + \text{RootsInZeroOne}(p_2)$;
14: **return** $m + m'$.

In Algorithm 5, at Line 1 we define $p_1(x) := x^d p(1/x)$ so that the roots of $p(x)$ in the range $]0, 1[$ are in an 1-to-1 correspondence with the roots of $p_1(x)$ in the range $]1, +\infty[$. The justification of this fact is similar to that of Algorithm 4. At Line 2, we compute $p_2(x)$ the Taylor shift by 1 of $p_1(x)$, so that now the roots of $p(x)$ in the range $]0, 1[$ are in an 1-to-1 correspondence with the roots of $p_2(x)$ in the range $]1, +\infty[$. Thus we can apply Descartes' rule to $p_2(x)$ in order to estimate the number of real roots of p in the range $]0, 1[$. More precisely, let v be the number of sign changes in $p_2(x)$. We know from Theorem 1 that if $v \leq 1$ holds then p admits exactly v real roots in the range $]0, 1[$. This fact is implemented at Line 4. If $v > 1$ holds, then we search for real roots of p in $]0, 1/2[$, in $]1/2, 1[$ at $x = 1/2$. This is done, via the polynomials $p_1(x)$ and $p_2(x)$ (defined at Lines 6 and 7), by two recursive calls (at Lines 12 and 13) and by testing whether x divides p_2 or not (at Line 8).

2.5 Taylor shift

The *Taylor shift* is a core routine of real root isolation algorithms. As we saw before, the VCA Algorithm reduces the problem of isolating the real roots of a univariate squarefree $p(x) \in \mathbb{Q}(x)$ to that of computing the coefficients of $p(x+1)$ in the monomial basis. This latter computation is referred as the *Taylor shift* of p by 1.

More generally, let $p = \sum_{0 \le i \le n} c_i x^i \in \mathbb{Q}(x)$ and let $a \in \mathbb{Q}$. Computing the coefficients of $p(x+a)$ in the monomial basis, say $g_0, \ldots, g_n \in Z$, such that we have

$$p(x+a) = \sum_{0 \le k \le n} g_k \, x^k,$$

is refered as the *Taylor shift* of p by a. The following proposition states an expression of the coefficients $g_0, \ldots, g_n \in \mathbb{Q}$ as functions of the coefficients $c_0, c_1, \ldots, c_n$ and a.

Proposition 1. *With the above notation, we have for each $i = 0 \cdots n$,*

$$g_i = \sum\nolimits_{j=0}^{n-i} c_{i+j} \binom{i+j}{i} a^j. \tag{2.6}$$

Proof. Recall $p(x) = \sum_{i=0}^{n} c_i x^i$ and $g(x) = \sum_{i=0}^{n} g_i x^i$ where $g(x) = p(x+a)$. We have:

$$p(x+a) \;=\; c_0 + c_1(x+a) + c_2(x+a)^2 + \cdots + c_n(x+a)^n. \tag{2.7}$$

From the above expression, we can easily deduce g_0, g_1, g_n:

$$\begin{array}{rcl} g_0 & = & c_0 + c_1 a + c_2 a^2 + \cdots + c_n a^n \\ g_1 & = & c_1 + 2ac_2 + 3c_3 a^2 + \cdots + n c_n a^{n-1} \\ & \vdots & \\ g_n & = & c_n \end{array} \tag{2.8}$$

For the general case, that is for g_i, we need to understand what is the contribution of each term from the following expression:

$$c_i(x+a)^i + c_{i+1}(x+a)^{i+1} + \cdots + c_{i+j}(x+a)^{i+j} + \cdots + c_n(x+a)^n. \tag{2.9}$$

Recall the binomial formula:

$$(u+v)^s \;=\; \sum\nolimits_{k=0}^{s} \binom{s}{k} u^k v^{s-k}. \tag{2.10}$$

This shows that the coefficient of x^i in $c_{i+j}(x+a)^{i+j}$ is $c_{i+j}\binom{i+j}{i}a^j$. Therefore, we have:

$$g_i \;=\; \sum_{j=0}^{n-i} c_{i+j}\binom{i+j}{i}a^j. \tag{2.11}$$

□

An important special case is $a = \pm 1$ [22]. There are classical methods to compute the coefficients $g_0, \ldots, g_n$: the famous *Horner Method* (see Section 2.5.1), *Shaw and Traub's method* (see [22]) and *multiplication-free methods* such as the *Pascal Triangle Method* (see Section 2.5.2). This latter is at the basis of two parallel algorithms presented in [6] and that we review in Sections 3.1 and 4.1.

2.5.1 Horner's method for Taylor shift by a

Let p and g as above. Horner's rule relies on the following re-combination of terms:

$$\begin{array}{rcl} g(x) & = & p(x+a) \\ & = & c_0 + (x+a)\,(c_1 + \cdots + c_n\,(x+a)^{n-1}) \end{array} \tag{2.12}$$

whose purpose is to evaluate any univariate polynomial of degree n within $2\,n$ additions and multiplications. Let us write:

$$g^n(x) = g(x) \;\text{ and }\; g^{n-1} = c_1 + \cdots + c_n\,(x+a).$$

Then we have:

$$g^n(x) = c_0 + (x+a)g^{n-1}(x) \tag{2.13}$$

Therefore, if $g^{n-1}(x)$ has been expanded on the monomial basis, we deduce a monomial basis expansion of g^n. The number $T(n)$ of arithmetic operations is thus ruled by

$$T(n) = T(n-1) + 2n + n,$$

which implies that Horner's rule requires $3/2n^2 + 3/2n + 1$ additions and multiplications. See [22] for details.

2.5.2 Taylor shift by 1 via Pascal's Triangle construction

From now on, we restrict ourselves to the case $a = 1$ which is what we need for the purpose of real root isolation. Formula (2.13) becomes:

$$g^n(x) = c_0 + (x+1)g^{n-1}(x).$$

This shows that the term of order i in $g^n(x)$ is obtained by adding the term of degree i from $g^{n-1}(x)$ (if any) and the term of degree $i-1$ from $g^{n-1}(x)$. This gives rise to a multiplication-free algorithm which boils down to construct a Pascal Triangle, see Figure 2.1. The number of additions necessary to compute $g_0, \ldots, g_n$ is then equal to the number of entries that are filled in the triangle, which is $(n+2)(n+1)/2$.

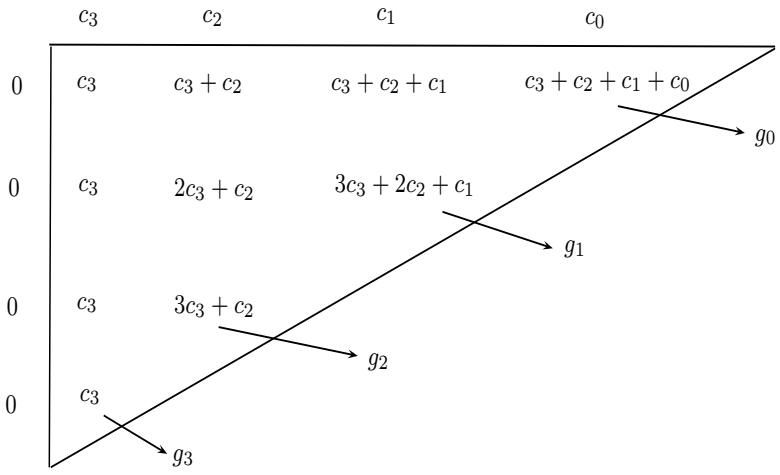

Figure 2.1: Pascal Triangle.

The Pascal Triangle can be computed in different ways. In this thesis, following [6] we consider two schemes that we call *divide and conquer* and *blocking*. The former one is discussed in Chapters 3 and 6 while the latter in Chapters 4, 7.

2.6 Cache memories and cache complexity

2.6.1 Cache memories

A cache memory is a small memory used by the central processing unit (CPU) of a computer. The access time of this cache memory is very fast compared to the access time of the main memory. Data is brought into the cache memory by the CPU before it can be used by the CPU registers. Once in cache, data can be reused for several

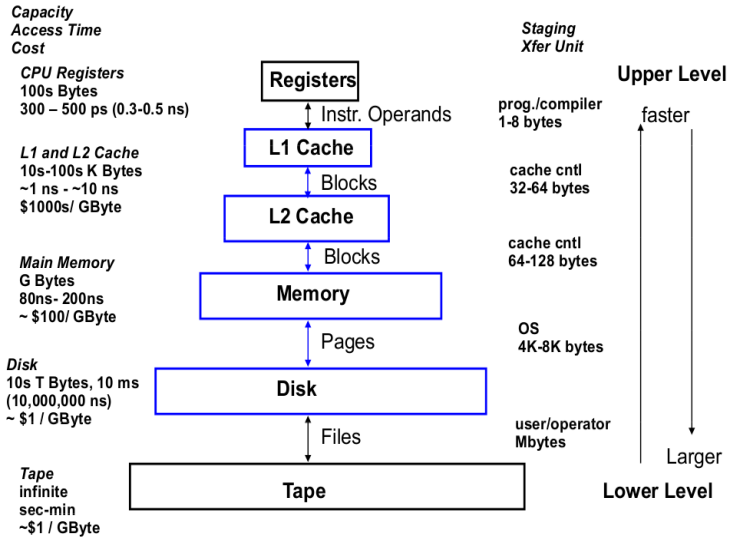

Figure 2.2: Memory hierarchy in a computer

computations by the CPU. When a data item required by the CPU is found in the cache memory, we say that we have a *cache hit*, otherwise we have *cache miss*.

Using cache memories effectively can reduce memory access times in a spectacular manner. C or FORTRAN programs implementing fundamental operations such as matrix multiplication can be accelerated by two orders of magnitude[1] *simply* by optimizing the use of cache memories. Modern desktops and laptops have typically two levels of cache.

L1-cache: L1-cache is the fastest cache and it usually comes within the processor chip itself. The L1 cache typically ranges in size from 8KB to 64KB and uses the high-speed SRAM (static RAM) instead of the slower and cheaper DRAM (dynamic RAM) used for main memory.

L2-cache: L2-cache is bigger than L1-cache and it sits between L1 and RAM. It's size is typically 64KB to 4MB.

Multi-level caches generally operate by checking for data in the L1 cache; if found, the processor proceeds at high speed. If the data is not in L1 cache, the next larger cache (L2) is checked before main memory is checked.

Data is moved between memory levels in *cache lines*, also called *blocks* and which typically hold 64 to 256 bytes. This implies that when the CPU loads a value (say an integer of a floating point number) from a lower level memory to a higher level

[1] `http://www.csd.uwo.ca/ moreno//Publications/SHARCNET_Tutorial.pdf`

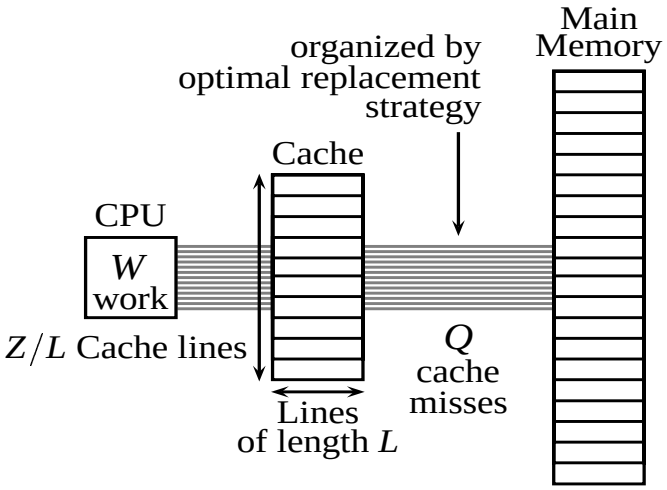

Figure 2.3: Ideal cache model

memory, several variables are actually loaded. This mechanism suggests that there are two properties for a program to perform well toward avoiding unnecessary and costly memory operations (loads and stores).

Temporal locality: This refers to the reuse of specific data within relatively small time durations.

Spatial locality: This refers to the use of data elements within relatively close storage locations.

2.6.2 Cache complexity

The ideal cache model, introduced in [10], assumes a computer system with a two-level memory hierarchy where the first level is an ideal (data) cache of Z words and the second level is an arbitrarily large main memory. The cache is partitioned into Z/L *cache lines* where L is the length of each cache line, in other words, each cache line can hold L consecutive words which are always moved together between the cache and the main memory. Cache designers usually use $L > 1$ to achieve *spatial locality*. It is generally assumed that the cache Z is much larger than L. More precisely,

$$Z = \Omega(L^2).$$

This type of cache is called *tall* cache, which is always the case in practice.

When a word required by the processor is found in cache, we say (as in the previous section) that we have a *cache hit*. Otherwise, we say that we have a *cache miss* and

the line can be fetched in any available block into in the cache. This mapping from main memory to cache is called *full associativity*. If the cache is full a cache line must be evicted. In the ideal cache model, the cache line whose next access is furthest in the future is replaced [1]: this is called an *optimal off-line strategy of replacing*.

For an algorithm with an input of size n, the ideal-cache model uses two complexity measures:

- the *work complexity* $W(n)$, which is its conventional running time in a RAM model.
- the *cache complexity* $Q(n; Z, L)$, the number of cache misses it incurs (as a function of the size Z and line length L of the ideal cache).
- When Z and L are clear from context, we simply write $Q(n)$ instead of $Q(n; Z, L)$.

An algorithm is said to be *cache aware* if its behavior (and thus performances) can be tuned (and thus depend on) on the particular cache size and line length of the targeted machine. Otherwise the algorithm is *cache oblivious*.

2.7 Multicore architecture

A *multi-core processor* is an integrated circuit to which two or more individual processors (called cores in this sense) have been attached. In a many-core processor the number of cores is large enough that traditional multi-processor techniques are no longer efficient. Cores on a multi-core implement the same architecture features as single-core systems such as instruction pipeline parallelism (ILP), vector-processing, SIMD or multi-threading. Many applications do not realize yet large speedup factors: parallelizing algorithms and software is a major on-going research area.

There are two important issues related to multicore architectures that may significantly reduce performances.

True sharing cache misses occur whenever two processors access the same data word. True sharing requires the processors involved to explicitly synchronize with each other to ensure program correctness. Programs with high temporal locality tend to have less true sharing.

False sharing occur whenever different processors use different data that happen to be co-located on the same cache line. Enhancing spatial locality often minimizes false sharing

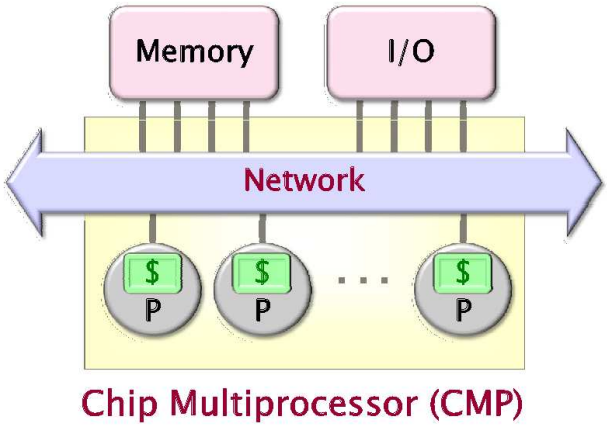

Figure 2.4: Multicore architecture

High levels of false or true sharing and synchronization can easily overwhelm the advantage of parallelism. See *Data and Computation Transformations for Multiprocessors* by J.M. Anderson, S.P. Amarasinghe and M.S. Lam `http://suif.stanford.edu/papers/anderson95/paper.html`

Another important cause of poor performances in multi-threaded programs on multicore architectures is the fact that access to the main memory (RAM) is serialized. More precisely, the RAM memory controller can serve only one load or store request at a time. However, CPUs in a multicore can issue those requests faster than the memory controller can process them. As a result of this *memory contention* phenomenon, the performances of a multi-threaded program can be dramatically reduced up to a point that the potential benefits of concurrent execution are annihilated.

2.8 The fork-join parallelism model and Cilk++

2.8.1 The Cilk++ concurrency platform

`Cilk` has been developed since 1994 at the Massachusetts Technology Institute (MIT) by *Prof. Charles E. Leiserson* and his research group, in particular by *Matteo Frigo*. Besides being used for research and teaching, `Cilk` was the system used to code the three world-class chess programs: Tech, Socrates, and Cilkchess. Over the years, the implementations of `Cilk` have run on computers ranging from networks of Linux laptops to an 1824-nodes Intel Paragon. From 2007 to 2009 Cilk has lead to `Cilk++`, developed by `Cilk Arts`, an MIT spin-off, which was acquired by `Intel` in July

2009 and became Cilk Plus, see `http://www.cilk.com/` Today, `Cilk++` can be freely downloaded at

`http://software.intel.com/en-us/articles/download-intel-cilk-sdk/`

`Cilk` is still developed at MIT by Prof. Charles E. Leiserson and his research group, see the page:

`http://supertech.csail.mit.edu/cilk/`

`Cilk++` (resp. `Cilk`) is a small set of linguistic extensions to `C++` (resp. `C`) supporting *fork-join parallelism*. In the `Cilk++` program below, the named *child* function `cilk_spawn fib(n-1)` may execute in parallel with its *parent* executes `fib(n-2)`. The `Cilk++` keywords `cilk_spawn` and `cilk_sync` grant permissions for parallel execution. They do not command parallel execution.

```
int fib(int n) {
  if (n < 2) return n;
  int x, y;
  x = cilk_spawn fib(n-1);
  y = fib(n-2);
  cilk_sync;
  return x+y;
}
```

2.8.2 The fork-join parallelism model

A simple theoretical model for the parallel execution of a `Cilk++` program is a DAG (directed acyclic graph) where

- each vertex represents a *strand*, that is, a sequence of consecutive instructions, to be executed serially.
- each edge indicates a chronological dependency between two strands.

This DAG is called *instructions stream DAG*. See Figure 2.5 for an example and [3] for details.

Three performance measures are naturally associated to a `Cilk++` and, more generally, to an instruction stream DAG.

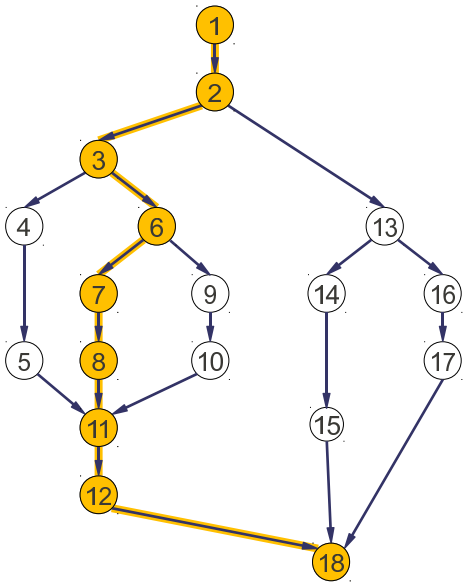

Figure 2.5: A directed acyclic graph (dag) representing the execution of a multithreaded program. Each vertex represents a strand and each edges represents a dependency between two strands.

T_p is the minimum running time on p processors

T_1 is called the *work*, that is, the sum of the number of instructions at each vertex in the DAG,

T_∞ is the minimum running time with infinitely many processors, called the *span*.

Assuming that all strands run in unit time (assuming also no cache issues, no interprocessor costs) the longest path in the DAG from the initial strand to a final strand is equal to T_∞. For this reason, T_∞ is also referred to as the *critical path length*.

Since, in the best case, p processors can do p works per unit of time, we have: $T_p \geq T_1/p$, which is often referred as the *work law*.

Since $T_p < T_\infty$ would contradict the definitions of T_p and T_∞, we have $T_p \geq T_\infty$, which is often referred as the *span law*.

The quantity T_1/T_p is called the *speedup on p processors*. A parallel program execution can have:

- *linear speedup*: $T_1/T_P = \Theta(p)$
- *superlinear speedup*: $T_1/T_P = \omega(p)$ (not possible in this model, though it is possible in others)

- *sublinear speedup*: $T_1/T_P = o(p)$

By definition, the *parallelism* of an instruction stream DAG is the ratio work to span, namely T_1/T_∞. This represents the average number of strands which can be run concurrently along the critical path.

2.8.3 Work-stealing scheduling

Cilk++ runtime system has work stealing scheduler which is reliable in sense that it can dynamically and automatically exploit an arbitrary number of available processor cores near optimally. When the Cilk++ runtime system starts up, it allocates as many system threads, called *workers* for the processors. When any subroutine is spawned, the activation frame is pushed to the bottom of the stack of the corresponding processor. When the child is returned to its parent, the parent's activation frame is popped of the stack. During the execution of the program, if any worker runs out of work, it "steals" work from (the top of) another worker's stack.

Assume that, for an application running with P processors:

- each strand executes in unit time,
- for almost all "parallel step" there are at least P strands to run,
- each processor is either working or stealing.

Then the `Cilk++` work-stealing scheduler achieves an expected running time as

$$T_P \leq T_1/P + O(T_\infty)$$

If the parallelism T_1/T_∞ is so large that it sufficiently exceeds P, then this bound provides a nearly prefect linear speed up. Assuming $T_1/T_\infty \gg P$, or equivalently $T_1/P \gg T_\infty$, the inequality leads to $T_P \approx T_1/P$. `Cilk++` estimates T_p as $T_p = T_1/p + 1.7S_b$ where S_b is the *burdened span*, that is, 15000 instructions times the number of spawns along the critical path. See Sections 2.8.4 and 2.8.5 for details.

2.8.4 Cilk++ execution model

This section is essentially adapted from the `Cilk++` Programming guide which can be found at `http://software.intel.com/en-us/articles/intel-cilk-plus/`. Recall that the instruction stream DAG of a `Cilk++` program does not depend on the

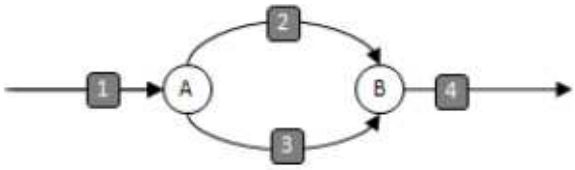

Figure 2.6: Cilk++ execution model dag.

number of processors. The execution model describes how the runtime scheduler maps strands to workers. Consider the following `Cilk++` program fragment:

```
do_init_stuff();        // execute strand 1
cilk_spawn func3();     // spawn strand 3 (the "child")
do_more_stuff();        // execute strand 2 (the "continuation")
cilk_sync;
do_final_stuff;         // execute strand 4
```

DAG for the code is showed in Figure 2.6.

If there is more than one worker available, there are two ways this program may execute:

- the entire program may execute on a single worker, or
- the scheduler may choose to execute strands (2) and (3) on different workers.

If there is a worker available, then strand (2) (the "**continuation**", we refer this as continuation since this strand continues from where the parent strand was spawned) may execute on the current (parent) worker or on a different worker (latter situation is referred as "work stealing").

In our Figure 2.7 we have showed that the work has been stolen from the parent worker and a second worker will begin executing the continuation, strand (2). The first worker (parent) will proceed to the synchronization at (B). Here, we indicate the second worker by illustrating strand (2) with a dotted line. After the synchronization, strand (4) may continue on either worker.

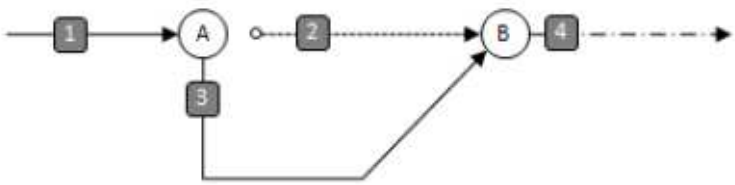

Figure 2.7: Cilk++ execution model dag.

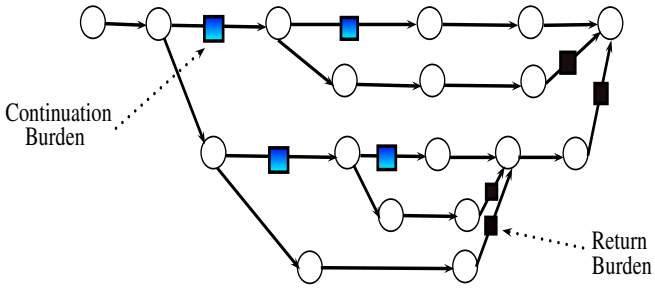

Figure 2.8: Burdened dag due to continuation and return burden

2.8.5 Burdened parallelism

When work is stolen, there is a cost for migrating the stolen tasks work set. There is also a cost for the continuation and return edges (in the DAG) which reflects overheads due to scheduling. The performance analyzer `Cilkview` [13] assumes that, for each spawn, a burden of 15,000 instruction cycles is created due to locks, malloc, cache warmup, etc.

Figure 2.5 shows burden on each continuation edge on the DAG. The ***burdened span*** is the longest path in the burdened dag. The migration cost can incorporate the bound $T_P \leq T_1/P + O(T_\infty)$ as

$$T_P \leq T_1/P + 2\delta\hat{T_\infty}$$

where, δ is the span coefficient and $\hat{T_\infty}$ is the burdened span while the program is running on P processor. The burden parallelism is computed as $T_1/\hat{T_\infty}$. See [13] for details.

2.8.6 Cilk_for

The following section is also essentially repeating the `Cilk++` Programming guide which can be found at `http://software.intel.com/en-us/articles/`

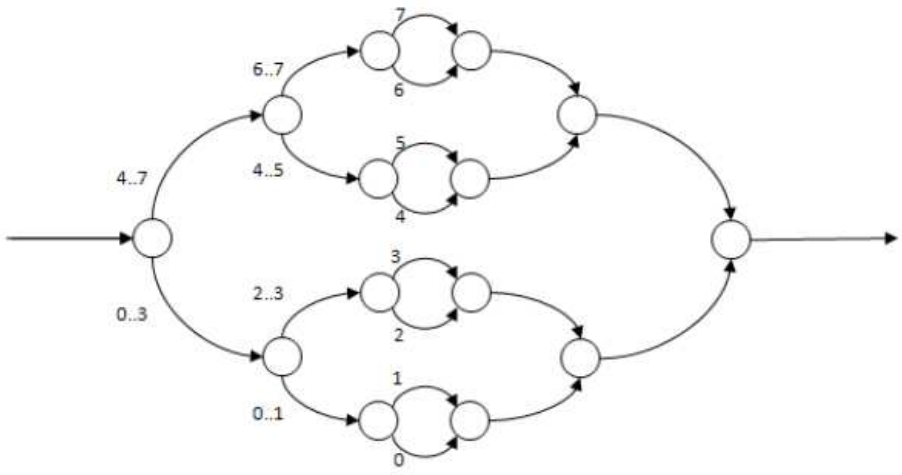

Figure 2.9: DAG for *cilk_for*.

`intel-cilk-plus/`. A *cilk_for* loop is a replacement for the normal `C++ ‘‘for loop’’` that permits loop iterations to run in parallel. A Sample *cilk_for* loop is like:

```
cilk_for (int i = begin; i < end; i += 2){
     f(i);
}
```

Using *cilk_for* is not the same as spawning each loop iteration. In fact, the `Cilk++` compiler converts the loop body into a function that is called recursively using a divide and conquer strategy, which allows the `Cilk++` scheduler to provide significantly better performance. The difference between a *cilk_for* and a `for` loop spawning each loop iteration can be seen clearly using instruction stream DAGs.

First, the DAG for a *cilk_for*, in Figure 2.9, assuming $N = 8$ iterations. The numbers labeling the strands indicate which loop iteration is handled by each strand. Note that at each division of work, half of the remaining work is done by the the child thread and half by the continuation. Importantly, the overhead of both the loop itself and of spawning new work is divided evenly along with the cost of the loop body.

If each iteration takes the same amount of time T to execute, then the span is $log_2(N)\,T$, or $3 * T$ for 8 iterations. The runtime behavior is well balanced regardless of the number of iterations or number of workers.

But, in the case of spawning loop iteration, the work is not well balanced, because each child does the work of only one iteration before incurring the scheduling overhead inherent to entering a sync. For a short loop, or a loop in which the work in the body

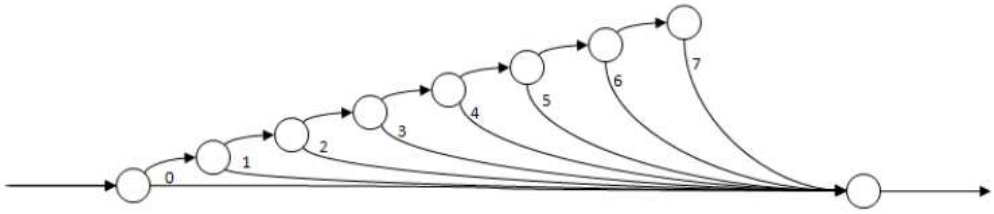

Figure 2.10: DAG for *cilkspawn*.

is much greater than the control and spawn overhead, there will be little measurable performance difference. However, for a loop of many cheap iterations, the overhead cost will overwhelm any advantage provided by parallelism. The DAG for a serial loop that spawns each iteration showed in Figure 2.10.

Chapter 3

Divide and Conquer Taylor shift: Static approach

Taylor shift computation, based on the Pascal Triangle construction, can be performed using different schemes. In this thesis, we consider two schemes that we call *divide and conquer* and *blocking*, following [5]. This chapter is dedicated to the former and the next chapter to the latter. Both chapters recall these schemes and provide complexity estimates for work, span and cache misses. These results already appear [5] but with sketches of proof, while we try here to make these proofs more complete.

We say that the algorithms of this chapter and the next one follow a static approach in the sense that they are not able to adapt themselves to the phenomenon of intermediate expression swell, studied in Chapter 5. On the contrary, the algorithms of Chapter 6 and 7 are *adaptive* (or *dynamic*), as they are able to dynamically change the granularity of their parallelism in order to improve performances.

3.1 Implementation scheme for static divide and conquer

Recall from Section 2.5.2 that the Taylor shift by 1 of a polynomial can be obtained via a Pascal Triangle construction. One can observe from Figure 3.1 that a Pascal Triangle can be constructed in a recursive manner: first computing the elements in the top-left square region then computing the elements of the two triangular regions. Moreover, one can observe that the two triangular regions can be evaluated concurrently. This recursive way of constructing Pascal Triangle is called *Divide and Conquer* method. This method uses a base case to determine until which point the

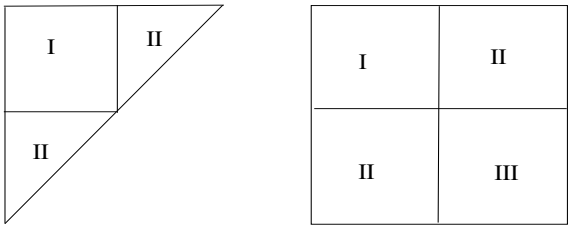

Figure 3.1: Divide and conquer Taylor shift.

triangular or the square regions will be divided into smaller regions. If this base size remains same for entire computation, then this divide and conquer process can be referred as *Static divide and conquer*. In this chapter we will focus only on static approach. Later in Chapter 6 we will discuss about the dynamic approach.

Figure 3.1 shows static divide and conquer in simplified fashion. The Pascal Triangle is divided into 3 regions, one tableau (region I) , and two triangles (region II) . These two triangle regions can work parallel. Tableau region is further divided into four regions I, II, II, III respectively. For tableau, the regions denoted as II can be computed concurrently. When they reach to base case, they stop doing division and everything is computed in a sequential manner. For static divide and conquer, base case should have to be at least of size 2, means it must contain at least 2 elements to compute.

3.1.1 Algorithms for Static Divide and Conquer

Let B be order of a block, where $B > 0$. For a polynomial of degree d, we have n number of inputs for Pascal Triangle, where $n = d + 1$.

Algorithm 6, `taylorShiftGeneral` is doing the task of recursively dividing each triangle into one square and two triangular regions. If $n \leq B$ then whole computation is done serially which is showed at Lines 1 and 2. In Line 5, Algorithm 7 is called which computes the square part. Lines 6 and 7 are two recursive calls with upper and lower triangles. When the triangles reach base case means no further division is required, then Algorithm 9 is called.

Algorithm 7, `tableauConstruction`, is for recursively dividing the square region (Tableau) until base case is reached. Like Algorithm 6, Algorithm 7 is also a recursive algorithm where base case is computed by Algorithm 8.

Algorithm 8, `tableauBaseInplace` works when the square region reaches to base

Algorithm 6: `taylorShiftGeneral`$(p[0 \dots n-1], q[0 \dots n-1], B)$

Input: $p[0 \dots n-1]$ is the coefficient array (dense representation) of a univariate polynomial $p(x)$ of degree d where $n = d+1$ ($a[i]$ is the coefficient of the term of degree i); $q[0 \dots n-1]$ is another array of length n, where all coefficients are initially zero; both $p[0 \dots n-1]$ and $q[0 \dots n-1]$ are overwritten; B is the base size (threshold).

Output: Coefficient array of the polynomial $p(x+1)$ stored in the array $p[0 \dots n-1]$ such that $a[i]$ is the coefficient of the term of degree i.

1: **if** $n \leq B$ **then**
2: | `taylorShiftBase`$(p[0, \dots, n-1], q[0, \dots, n-1])$;
3: **else**
4: | $m = \frac{n+1}{2}$;
5: | `tableauConstruction`$(p[0 \dots m-1], q[0 \dots m-1], B)$;
6: | **spawn** `taylorShiftGeneral`$(p[0 \dots m-1], q[m \dots n-1], B)$;
7: | **spawn** `taylorShiftGeneral`$(p[m \dots n-1], q[0 \dots m-1], B)$;
8: | **Sync**

Algorithm 7: `tableauConstruction`$(p[0 \dots m-1], q[0 \dots n-1], B)$

Input: Array $p[0 \dots n-1]$ of size m and array $q[0 \dots n-1]$ of size n; initially $p[0 \dots m-1]$ and $q[0 \dots n-1]$ contain the input coefficients; $p[0 \dots m-1]$ and $q[0 \dots n-1]$ are overwritten during the computations; B is the base size (threshold).

Output: Result of right edge of Tableau is stored on array $p[0 \dots m-1]$ and down edge of tableau is stored on array $q[0 \dots n-1]$.

1: **if** *($m \leq B$)* AND *($n \leq B$)* **then**
2: | `tableauBaseInplace`$(p[0 \dots m-1], q[0 \dots n-1])$;
3: **else**
4: | $i = \frac{m+1}{2}$;
5: | $j = \frac{n+1}{2}$;
6: | `tableauConstruction`$(p[0 \dots i-1], q[0 \dots j-1], B)$;
7: | **spawn** `tableauConstruction`$(p[0 \dots i-1], q[j \dots n-1], B)$;
8: | **spawn** `tableauConstruction`$(p[i \dots m-1], q[0 \dots j-1], B)$;
9: | **sync**
10: | `tableauConstruction`$(p[i \dots m-1], q[j \dots n-1], B)$;

case and no further division is required. Here every computation is done in serial manner.

Algorithm 8: `tableauBaseInplace`$(p[0 \dots m-1], q[0 \dots n-1])$

Input: Array $p[0 \dots m-1]$ of size m and array $q[0 \dots n-1]$ of size n; initially $p[0 \dots m-1]$ and $q[0 \dots n-1]$ contain the input coefficients; $p[0 \dots m-1]$ and $q[0 \dots n-1]$ are overwritten during the computations.

Output: Result of right edge of Tableau is stored on array $p[0 \dots m-1]$ and down edge of tableau is stored on array $q[0 \dots n-1]$.

```
2: for i = 0 to n − 1 do
4:     p[0] = p[0] + q[i];
6:     for j = 1 to m − 1 do
7:         p[j] = p[j] + q[j − 1];
9:     q[i] = p[m − 1];
```

Algorithm 9 `taylorShiftBase` computes triangles in base case.

Algorithm 9: `taylorShiftBase`$(p[0 \dots n-1], q[0 \dots n-1])$

Input: Array $p[0 \dots n-1]$ and array $q[0 \dots n-1]$ of size n; initially $p[0 \dots n-1]$ and $q[0 \dots n-1]$ contain the input coefficients.

Output: Coefficient array of the polynomial $p(x+1)$ stored in the array $p[0 \dots n-1]$ such that $a[i]$ is the coefficient of the term of degree i.

```
2: for i = 0 to n − 1 do
4:     p[0] = p[0] + q[i];
6:     for j = 1 to n − i − 1 do
7:         p[j] = p[j] + q[j − 1];
```

3.1.2 Cases to consider in divide and conquer

For the example in Figure 3.2, we can see that there are two types of cases for Divide and Conquer method, *Regular case* (when n is power of 2) and *Irregular case* (when n is not a power of 2). Both for regular and irregular case, the tableau (square part) is computed first. For the square part, it is divided into four regions $L_{1,1}, L_{2,1}, L_{2,2}$ and $L_{3,1}$. Region $L_{1,1}$ will be computed first. Then region $L_{2,1}$ and region $L_{2,2}$ both can be done concurrently. After that region $L_{3,1}$ is computed. When square region is finished computing, the smaller triangles can be computed in parallel. From Figure 3.2, we can see that the lower triangle is divided into 3 more regions, the tableau region $L_{4,1}$ and 2 triangle regions $L_{5,1}$ and $L_{5,2}$. Upper triangle is also divided into 3 regions,

tableau region $L_{4,2}$, and two triangles $L_{5,3}$ and $L_{5,4}$ respectively. The square regions for both triangles $L_{4,1}$ and $L_{4,2}$ can be done concurrently. Then the triangle regions $L_{5,1}, L_{5,2}, L_{5,3}, L_{5,4}$ are done parallel.

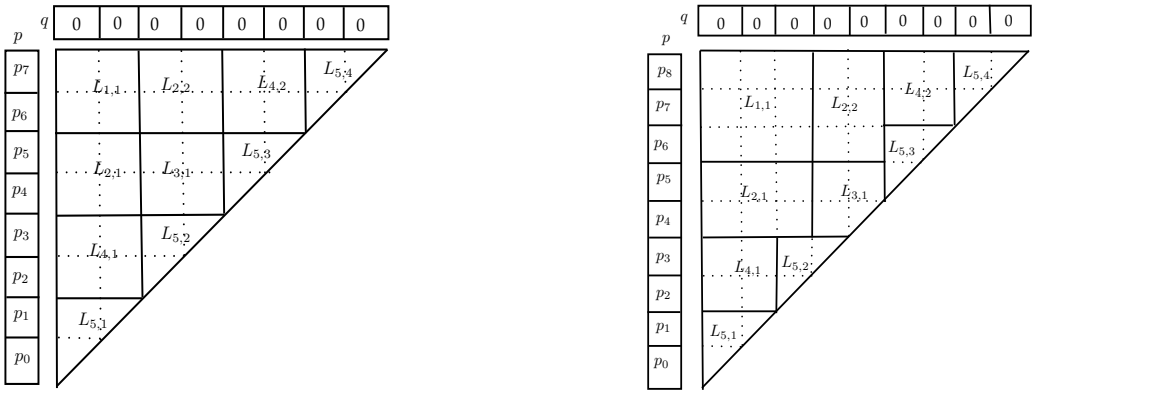

(a) Regular case: n is a power of 2 **(b) Irregular case: n is not a power of 2**

Figure 3.2: Case illustration for implementing Dnc strategy

3.2 Work, span and parallelism estimates

Our work, space and parallelism estimates for the divide and conquer approach follow the fork-join parallelism model discussed in Chapter 2.

Let $W_s(n)$ (resp. $W_T(n)$) the work of the square (resp. triangle) construction and let $S_s(n)$ (resp. $S_T(n)$) the span of the square (resp. triangle) construction.

The work $W_s(n)$ required for filling in the tableau satisfies

$$W_s(n) = 4W_S(n/2) + \Theta(1) \tag{3.1}$$

Where, $n > 1$. Applying the *Master Theorem*[1] which implies:

$$W_s(n) = \Theta(n^2) \tag{3.2}$$

For same construction the span is :

$$S_s(n) = 3S_s(n/2) + \Theta(1) \tag{3.3}$$

[1] http://en.wikipedia.org/wiki/Master_theorem

Where $n > 1$ and applying *Master Theorem* which leads to:

$$S_s(n) = \Theta(n^{log_2 3}) \tag{3.4}$$

For a Pascal Triangle, the work $W_T(n)$ is:

$$W_T(n) = 2W_T(n/2) + W_S(n/2). \tag{3.5}$$

Applying the *Master Theorem* yields:

$$W_T(n) = \Theta(n^2). \tag{3.6}$$

And span satisfies:

$$S_T(n) = S_T(n/2) + S_s(n) \tag{3.7}$$

which implies:

$$S_T(n) = \Theta(n^{log_2 3}). \tag{3.8}$$

Therefore, for both constructions the parallelism is about $\Theta(n^{0.45})$. For more details see at [5]

3.3 Space complexity estimate

Consider first the sequential algorithm. One can observe that, at any point of the construction of the Pascal's Triangle, the knowledge of $2n$, and only $2n$, integers (with $n = d + 1$) is needed in order to continue the construction until its completion. Moreover, the whole algorithm can be executed in place within the space allocated to the input $2n$ integers. At completion, the output n integers can be found in this allocated space, most likely in its first n slots.

The same property is easy to prove for the divide and conquer approach. To do so, one first establishes by induction a similar property for the two-way tableau construction, see Figure 3.1. Then, one proves by induction the desired property for the divide-and-conquer approach of the Pascal's Triangle depicted by Figure 3.1.

Finally, we conclude that the divide and conquer approach can be executed in place using an aggregate of $2n$ integers. Observe that, in order to obtain, a bit size complexity estimate, one would need to take the growth of the intermediate coefficients into account, see Chapter 5. If we assume that each input coefficient has bit size H or less, then one can check that the whole Pascal's Triangle construction

can be done within $2n(H+n)$ bits. Indeed, each output coefficient is computed from the input coefficients by n additions.

3.4 Cache complexity estimate

In their paper Changbo Chen, Marc Moreno Maza and Yuzen Xie established the following proposition [5]. Note that the assumption is realistic only when n and the coefficients of the input polynomial are small enough.

Proposition 2. *Assume that each input, output or intermediate coefficient is stored in constant space. In the* ideal cache model *[10], Algorithm 7 incurs* $\Theta(\frac{n}{L} + n^2/(ZL))$ *cache misses, which is optimal.*

Proof. Suppose, the cache size is of Z words and each cache line has L words. Given an input array of length n we need to find out a cache complexity upper bound for the two routines sketched by Figure 3.1. Let $Q_T(n)$ and $Q_S(n)$ be the number of cache misses incurred by the "triangle" and "square" routines.

Since Algorithm 7 can be run in space $2n$, we deduce that, for n small enough, the whole computation fits in cache (i.e. only cold misses occur). Therefore there exists a real constant $\alpha > 0$ such that we have:

$$Q_T(n) \leq \begin{cases} 2n/L + 1 & \text{if } n \leq \alpha Z \\ 2Q_T(\frac{n}{2}) + Q_S(n) & \text{otherwise,} \end{cases} \tag{3.9}$$

and

$$Q_S(n) \leq \begin{cases} 2n/L + 1 & \text{if } n \leq \alpha Z \\ 4Q_S(\frac{n}{2}) + \Theta(1) & \text{otherwise} \end{cases} \tag{3.10}$$

We first solve Equation (3.10). Expand this formula, we have:

$$\begin{aligned} Q_s(n) &\leq 4\Big(4Q_s(\tfrac{n}{4}) + \Theta(1)\Big) + \Theta(1) \\ &\leq 4\Big(4\Big(4Q_s(\tfrac{n}{8}) + \Theta(1)\Big) + \Theta(1)\Big) + \Theta(1) \end{aligned} \tag{3.11}$$

Enrolling shows that there exists an integer k such that we have :

$$Q_S(n) \leq 4^k \left(\frac{2\alpha Z}{L} + 1\right) + \sum\nolimits_{j=0}^{k-1} 4^j \Theta(1), \tag{3.12}$$

where k is the smallest number of "recursive levels" necessary such that each sub-

problem fits in cache. This number e is given by:

$$k \;=\; \lceil \log_2 \Big(\frac{n}{\alpha Z}\Big) \rceil. \tag{3.13}$$

The $\sum_{j=0}^{k-1} 4^j \Theta(1)$ of Equation (3.17) can be simplified using the well-known formula:

$$1 + q + q^2 + \cdots + q^{e-1} = \frac{-1 + q^e}{-1 + q}.$$

So, $\sum_{j=0}^{k-1} 4^j \Theta(1)$ becomes $\Theta(4^k)$ and thus the Equation (3.17) becomes

$$\begin{array}{rcl} Q_S(n) & \leq & 4^k \left(\frac{2\alpha Z}{L} + 1\right) + \Theta(4^k) \\ & \leq & \Theta(4^k) \left(\frac{2\alpha Z}{L} + 2\right) \end{array} \tag{3.14}$$

From Equation (3.13) we obtain the value of k and replace it in Equation (3.14), thus we have :

$$\begin{array}{rcl} Q_s(n) & \in & O\left(4^{log_2(\frac{n}{\alpha Z})} \left(\frac{2\alpha Z}{L} + 2\right)\right) \\ & \in & O\left((\frac{n}{\alpha Z})^2 \left(\frac{2\alpha Z}{L} + 2\right)\right) \\ & \in & O\left(\frac{2n^2}{\alpha Z L} + \frac{2n^2}{\alpha^2 Z^2}\right) \end{array} \tag{3.15}$$

After simplification we obtain :

$$Q_S(n) \in O(\frac{n^2}{ZL} + \frac{n^2}{Z^2}). \tag{3.16}$$

Now we solve for $Q_T(n)$ from Equation(3.9) we proceed in the same way just like Equation(3.10) and after simplification we get :

$$\begin{array}{rcl} Q_T(n) & \leq & 2^k Q_T\left(\frac{n}{2^k}\right) + \sum_{j=0}^{k-1} 2^j Q_S(\frac{n}{2^j}) \\ & \leq & 2^k(\frac{2\alpha Z}{L} + 1) + \sum_{j=0}^{k-1} 2^j (\frac{n}{2^j})^2 (\frac{1}{ZL} + \frac{1}{Z^2}) \\ & \leq & \frac{n}{\alpha Z}(\frac{2Z}{L} + 1) + \sum_{j=0}^{k-1} 2^{-j} (\frac{n^2}{ZL} + \frac{n^2}{Z^2}) \\ & \leq & \frac{n}{\alpha Z}(\frac{2Z}{L} + 1) + 2(\frac{n^2}{ZL} + \frac{n^2}{Z^2}) \\ & \leq & \frac{2n}{\alpha L} + \frac{n}{\alpha Z} + 2(\frac{n^2}{ZL} + \frac{n^2}{Z^2}). \end{array} \tag{3.17}$$

Which is actually

$$Q_s(n) \;\in\; O\left(\frac{n}{L} + \frac{n}{Z} + \frac{n^2}{ZL} + \frac{n^2}{Z^2}\right) \tag{3.18}$$

Using the tall cache assumption, that is, $Z \in \Omega(L^2)$, the above expression becomes

$$Q_s(n) \;\in\; O\left(\frac{n}{L} + \frac{n^2}{ZL}\right) \tag{3.19}$$

The optimality of this cache complexity result follows from the bound of J.W. Hong and H.T. Kung in their STOCS'81 paper "I/O complexity: the red-blue pebble game" [14]. □

Chapter 4

Blocking Taylor shift: Static approach

In this chapter, we describe and explain *Blocking* method which is an alternate way of performing Taylor shift computation. In Section 4.1 , we give a preliminary idea of blocking. Implementation schemes with algorithms are discussed in Section 4.2. Section 4.3 decribes work, span and parallelism for blocking. Space complexity and cache complexity are discussed in Section 4.4 and Section 4.5 respectively.

4.1 Blocking strategy

Divide and Conquer strategy suffers from a relatively low parallelism. If we recall Figure 3.1, we can see that the computations in the two triangle regions are not started until the square region I is completed. But tableau parts of small triangular regions can be started before completion of region I. Figure 4.1 gives an idea of designing a Pascal Triangle by blocking method instead of doing divide and conquer.

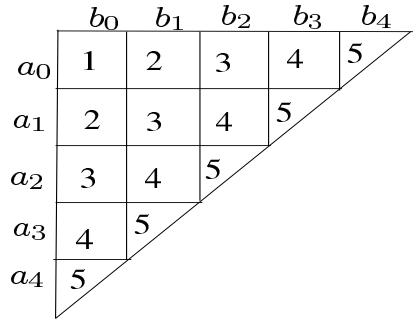

Figure 4.1: Blocking Strategy in Pascal Triangle

For more clarity, we can recall Figure 3.2 from chapter 3, we observe that region $L_{3,1}$ which is at down-right corner of tableau, is computed before region $L_{4,1}$ and $L_{4,2}$, which are the tableau regions of upper and lower triangles. But here we can compute all three regions concurrently since these three regions become available for computing in parallel at the same time. To overcome this limitation, a new approach is introduced called *Blocking method*.

In their paper [6] Changbo Chen, Marc Moreno Maza and Yuzhen Xie introduced a technique called *Blocking Strategy*, where the entire Pascal Triangle is partitioned into $B \times B$ blocks; the blocks are traversed as *diagonal band*. By *diagonal band* we mean rows from upper-left corner of triangle, such as "1", "$2, 2$", "$3, 3, 3$" etc. See Figure 4.1 .

4.2 Implementation scheme for static block

We consider two types of Blocking Strategy. One is *Regular case*, when the input n (where $n = d+1$, $d =$ degree of polynomial) is divisible by block size B, otherwise we call it *Irregular case*. The example in subfigure (a) of Figure 4.2, where $n = 9$ and $B = 3$, can be classified as regular case. Here the computation can be done in three steps. At first step, tableau $L_{1,1}$ is computed. At second step, two tableau $L_{2,1}$ and $L_{2,2}$ are computed in parallel. At last step, three small Pascal Triangles $L_{3,1}$, $L_{3,2}$, $L_{3,3}$ of are computed concurrently.

For discussing about irregular case we consider a situation when $n = 10$ and $B = 3$, see subfigure (b) of Figure 4.2 . After two diagonal rows of tableau from top left corner of triangle, a special case occurs here, we call it *polygonCase*. From Figure 4.2 we see that, three polygon cases $P_{3,1}$, $P_{3,2}$, $P_{3,3}$ (we call these special shapes as *Polygon* as their shape neither looks like 'Tableau' nor 'Triangle') occur after the tableau blocks are done. In last step, four Pascal Triangles are computed concurrently.

Figure 4.2 shows both cases for blocking strategy.

The pseudocode for Triangles in base case is described in Algorithm 10 and Tableau part is described in Algorithm 11. The special case *polygonCase* is described in Algorithm 12. Managing the computation of whole problem is done by Algorithm 13 for *regular case* and Algorithm 14 for *irregular case*.

Algorithm 10, `taylorBaseBlock` is called when the Pascal Triangle reaches to base case and every computation is done serially. Moreover, all the computations are done in place, within $2n$ space.

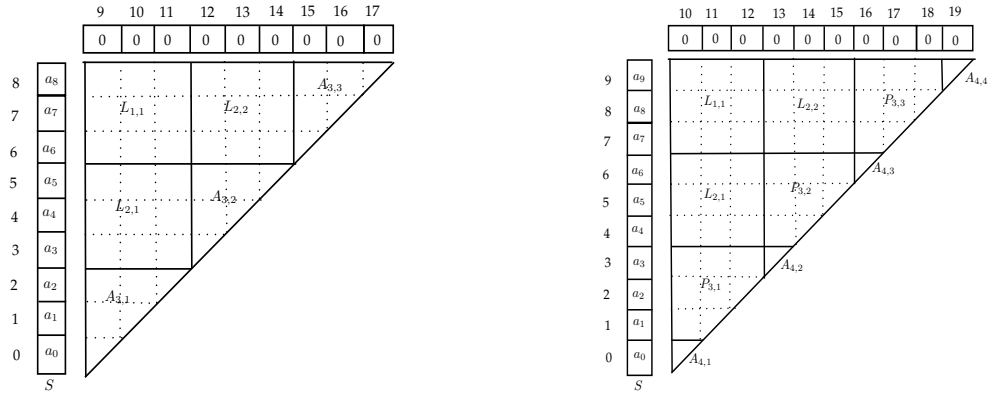

(a) Regular case: B divides n **(b) Irregular case: B does not divide n**

Figure 4.2: Case illustration for implementing blocking strategy

---

Algorithm 10: `taylorBaseBlock`$(a[0,\ldots,n-1],n)$

Input: $a[0\ldots n-1]$ is an array of size n; initially $a[0\ldots n-1]$ contains input coefficients; $a[0\ldots n-1]$ is overwritten during computations.

Output: Coefficient array of the polynomial $p(x+1)$ stored in the array $a[0\ldots n-1]$ such that $a[i]$ is the coefficient of the term of degree i.

```
2: for i = 0 to n − 1 do
4:     a[n − 1] = a[n − 1] + a[n + i];
6:     for j = n − 2 to i do
7:         a[j] = a[j] + a[j + 1];
8:         j = j − 1;
```

Algorithm 11, `tableauBaseBlock` is for tableau construction for blocking method. When a tableau region reaches to base case, the computation is done serially. In Algorithm 11, Line 2 and 3 compute first row of tableau. Line 4 to Line 7 is computing middle rows of tableau. Line 8 to Line 10 is computing last row of tableau. Results of the tableau is overwritten on input array, thus, the whole computation is done in $2n$ space.

Algorithm 11: `tableauBaseBlock`$(a[0,\ldots,n-1],n)$

Input: $a[0\ldots n-1]$ is an array of size n; initially $a[0\ldots n-1]$ contains input coefficients; $a[0\ldots n-1]$ is overwritten during computations.

Output: Coefficient array of the polynomial $p(x+1)$ stored in the array $a[0\ldots n-1]$.

```
1: m = 2n;
   ; /*first row                                                    */
2: for i = n to m − 1 do
3:     a[i] = a[i] + a[i − 1];
   ; /*middle rows                                                  */
4: for i = n − 2 to 1 do
5:     for j = 0 to n − 1 do
6:         a[i + j + 1] = a[i + j] + a[i + j + 2];
7:     i = i − 1;
   ; /*first element of last row                                    */
8: a[0] = a[0] + a[2];
   ; /*rest element of last row                                     */
9: for i = 1 to n − 1 do
10:    a[i] = a[i − 1] + a[i + 2];
   ; /*first element of first row                                   */
11: a[n] = a[n − 1];
```

In Algorithm 12, `polygonBase` is for polygon construction in blocking method. The special shape, which is neither a tableau, nor a triangle is handled by this algorithm. This type of special shape, which looks more like combination of "Rectangle" and "Trapezoid", can be divided into two areas. One is rectangle area at top of polygon and the other is trapezoidal area. In Algorithm 12, Line 2 to Line 7 calculates the rectangle rows. Rows with shape of trapezoid is computed from Line 8 to Line 12. Last row of polygon is computed at Line 13 to Line 15. Here results are also overwritten on input array, thus doing calculation in place.

Algorithm 12: `polygonBase`$(a[0,\ldots,n-1], n, r, k)$

Input: $a[0\ldots n-1]$ is an array of size n; initially $a[0\ldots n-1]$ contains input coefficients; $a[0\ldots n-1]$ is overwritten during computations; r is the reminder of (n mod B), k is the number of trapezoidal rows in polygon.

Output: Coefficient array of the polynomial $p(x+1)$ stored in the array $a[0\ldots n-1]$.

1: $m = 2n$;
; /*first row */
2: **for** $i = n$ *to* $m-1$ **do**
3: $\quad a[i] = a[i] + a[i-1]$;
; /*rectangle rows */
4: **for** $i = n-2$ *to* k **do**
5: $\quad$ **for** $j = 0$ *to* $n-1$ **do**
6: $\quad\quad a[i+j+1] = a[i+j] + a[i+j+2]$;
7: $\quad i = i-1$;
; /*trapezoid starts */
8: **for** $i = k-1$ *to* 1 **do**
9: $\quad a[k+1] = a[k+1] + a[i]$;
10: $\quad$ **for** $j = k+2$ *to* $n+i$ **do**
11: $\quad\quad a[j] = a[j] + a[j-1]$;
12: $\quad i = i-1$;
; /*first element of last row */
13: $a[0] = a[0] + a[k+1]$;
; /*rest element of last row */
14: **for** $i = 1$ *to* r **do**
15: $\quad a[i] = a[i-1] + a[i+k+1]$;

4.2.1 Regular case

When degree of a polynomial n is divisible by B, then regular case algorithm `staticBlockingRegular` will work. Algorithm 13 works for static block in regular case. Here, Line 6 to Line 12 is computing the tableau regions in parallel. Once the tableau part is done, Line 13 to Line 16 is calculating the triangle regions parallel.

All computations here are done in $2n$ space. It means the results are overwritten on input space.

Algorithm 13: `staticBlockingRegular`$(a[0 \dots n-1], n, B)$

Input: $a[0 \dots n-1]$ is the coefficient array (dense representation) of a univariate polynomial $p(x)$ of degree d where $n = d+1$ ($a[i]$ is the coefficient of the term of degree i); B is the base size (threshold).

Output: Coefficient array of the polynomial $p(x+1)$ stored in the array $a[0 \dots n-1]$ such that $a[i]$ is the coefficient of the term of degree i.

1: $m = 2n$;
2: $b[0, \dots, n-1] = a[0, \dots, n-1]$;
3: $b[n, \dots, m-1] = 0$;
4: $k = \frac{n}{B}$;
5: **if** $k > 1$ **then**
6: `tableauBaseBlock`$(b[n-B \dots n], B)$;
7: **for** $i = 2$ *to* $k-1$ **do**
8: **for** $j = 0$ *to* $i-2$ **do**
9: $t = n + (2j - i)B$;
10: **spawn** `tableauBaseBlock`$(b[t \dots t+B], B)$;
11: **spawn** `tableauBaseBlock`$(b[n + (i-2)B \dots n + iB - B], B)$;
12: **Sync**
13: **for** $i = 0$ *to* $k-2$ **do**
14: **spawn** `taylorBaseBlock`$(b[2iB \dots 2iB + B], B)$;
15: **spawn** `taylorBaseBlock`$(b[2(k-1)B \dots 2kB - B], B)$;
16: **Sync**
; `/*copy results from` b `to` a `*/`
17: **for** $i = 0$ *to* $k-1$ **do**
18: **for** $j = 0$ *to* $B-1$ **do**
19: $a[j + iB] = b[j + 2iB]$;

4.2.2 Irregular case

When input n is not divisible by B, then algorithm 14 will work. Algorithm 14 works for static block in irregular case. Here, Line 8 to Line 15 is computing the tableau regions in parallel. When the tableau part is done, Line 16 to Line 20 is calculating the special regions which we have named as *Polygon* regions. At the end, from Line 21 to Line 24 is computing triangle regions concurrently. Every computation is done here in place thus the result is stored on input array.

Algorithm 14: `staticBlockingIrregular`$(a[0 \dots n-1], n, B)$

Input: $a[0 \dots n-1]$ is the coefficient array (dense representation) of a univariate polynomial $p(x)$ of degree d where $n = d + 1$ ($a[i]$ is the coefficient of the term of degree i); B is the base size (threshold).

Output: Coefficient array of the polynomial $p(x+1)$ stored in the array $a[0 \dots n-1]$ such that $a[i]$ is the coefficient of the term of degree i.

```
1:  r = n mod B;
2:  q = n/B;
3:  m = 2n;
4:  k = B − r − 1 ;
5:  k = (k > 0)?k : 1;
6:  b[0, . . . , n − 1] = a[0, . . . , n − 1];
7:  b[n, . . . , m − 1] = 0;
8:  if q > 1 then
9:      tableauBaseBlock(b[n − B . . . n], B);
10:     for i = 2 to q − 1 do
11:         for j = 0 to i − 2 do
12:             t1 = n + (2j − i)B;
13:             spawn tableauBaseBlock(b[t1 . . . t1 + B], B);
14:         spawn tableauBaseBlock(b[n + (i − 2)B . . . n + iB − B], B);
15:         Sync
16: for i = 0 to q − 2 do
17:     t2 = n + (2i − q)B;
18:     spawn polygonBase(b[t2 . . . t2 + B], B, r, k);
19: spawn polygonBase(b[n + (q − 2)B . . . n + qB − B], B, r, k);
20: Sync
21: for i = 0 to q − 1 do
22:     spawn taylorBaseBlock(b[2iB . . . 2iB + r], r);
23: spawn taylorBaseBlock(b[2qB . . . 2qB + r], r);
24: Sync
25: Copy results from b[0 . . . n − 1] to a[0 . . . n − 1];
26: return a[0 . . . n − 1] ;
```

4.3 Work, span and parallelism estimates

Let B be the order of a block. Then the work for each block is $\Theta(B^2)$. If the number of elements is n, then there will be n/B "parallel steps" or we can say n/B *bands* (or diagonal rows) from the upper left corner of a triangle. Each of these bands has at most n/B blocks. Thus, we have $\Theta(n/B)^2$ blocks, hence the work for computing the Pascal Triangle is:

$$\begin{aligned} W_B(n) &\in \Theta(B^2) \times \Theta((n/B)^2) \\ &\in \Theta(n^2) \end{aligned} \tag{4.1}$$

As the span for each block is $\Theta(B^2)$, the span for the whole algorithm is:

$$\begin{aligned} S_B(n) &\in \Theta(B^2) \times n/B \\ &\in \Theta(Bn) \end{aligned} \tag{4.2}$$

The resultant parallelism is $\Theta(n^2/(Bn))$, which is $\Theta(n/B)$.

4.4 Space complexity estimate

For a $B \times B$ block, the computation is sequential and is done in place within $2B$ integers. At the k-th parallel step there are k blocks which requires $2kB$ integers in total. Therefore, the whole algorithm can be run with an aggregate of $2n$ integers (letting $k = n/B$). We observe that this analysis does not take into the growth of the intermediate coefficients. See Section 3.3 and Chapter 5 for more details on this subject.

4.5 Cache complexity estimate

Let α be the constant introduced in the cache complexity analysis of the divide and conquer approach. Assume that $B = \alpha Z$ holds. Then, the number of cache misses for each block is $2B/L + 1$ and the total number of cache misses is

$$Q(n) = \Theta((n/B)^2(2B/L + 1)) = \Theta(n^2/(BL)) = \Theta(n^2/(ZL)).$$

Therefore, provided that $B = \alpha Z$ holds, we retrieve the optimal cache complexity result established for the divide and conquer approach.

Chapter 5

Analysis of Workload in the Case of Integer Coefficients

5.1 Introduction

In the fork-join parallelism model, the work of each strand is assumed to have a unit cost. Under this assumption, the analyses that we conducted in the previous chapters show that the work for constructing Pascal's Triangle is quadratic in its order n. As long as all necessary additions can be performed correctly with machine integer arithmetic, this assumption is realistic. However, for n large enough, software integer arithmetic is required and this assumption is no longer acceptable.

More generally, this phenomenon invalidates our complexity analyses of the divide and conquer approach, and the blocking strategy for Taylor shift computations. To understand this, let us consider the divide and conquer approach for the Taylor shift, as described in Section 3.2. We revisit Figure 3.1 below.

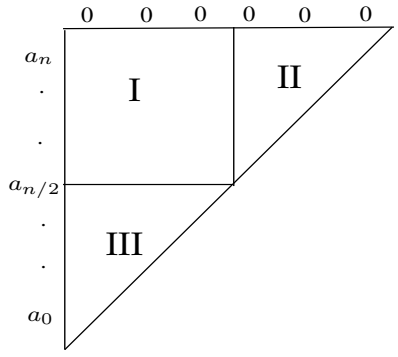

Figure 5.1: Pascal Triangle.

Under the assumption that each strand has unit work, Regions II and III in Figure 5.1 have the same work and span. Suppose now that we are using a 2-bit machine word machine. Then Region II requires more work (in terms of machine word operations) than Region III.

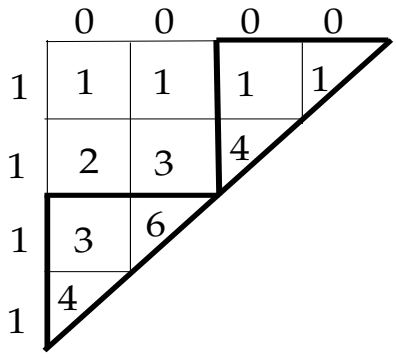

Figure 5.2: Example figure of DnC in Pascal Triangle

Suppose from now on that we are using a b-bit machine word machine, for an arbitrary integer $b > 1$. Consider two positive integers A and B in radix b representation

$$A = \sum_{i=0}^{s-1} A_i b^i \quad \text{and} \quad B = \sum_{i=0}^{t-1} B_i b^i,$$

with $A_{s-1} \neq 0, 0 \leq A_i < b$ and $B_{t-1} \neq 0, 0 \leq B_i < b$. The integers s and t are called the sizes of A and B, denoted respectively by $\#(A)$ and $\#(B)$. We clearly have

$$\max(\#(A), \#(B)) \leq \#(A + B) \leq \max(\#(A), \#(B)) + 1.$$

If A and B are random (with a uniform distribution), we have $\#(A + B) = \max(\#(A), \#(B)) + 1$ with a probability $1/2$. This explains the growth of the coefficients in the Pascal Triangle and thus, for n large enough, the unbalanced work between the two recursive calls in the divide and conquer construction of the Pascal Triangle.

The next two sections are dedicated to an analysis of this phenomenon and its impact on the work and span of parallel Taylor shift computations by means of the for the blocking strategy. We focus, indeed, on this scheme since its parallelism is higher than that of the divide and conquer startegy. In fact, the goal of this section is to obtain complexity estimates that will support an improved implementation of this scheme, reported in Section 7.

In Section 5.4, we analyse the parallelization overheads of the blocking strategy, which, in our opinion, brings some interesting and unexpected results. Finally, in Section 5.5, we turn our attention to locality issues. We establish formulas for chosing an initial block order B, and, if appropriate, changing this block order during the computations, so as to minimize cache misses.

5.2 Work for the blocking strategy

We consider a triangular grid as on Figure 3.1, where the top left corner is the origin, with Cartesian coordinates $(0, 0)$. The coefficient in the grid with coordinates (k, ℓ) (where k is the row index and ℓ is the column index) is denoted by $c_{k,\ell}$. The grid has n rows and n columns.

Initially, the coefficients satisfying either $k = 0$ or $\ell = 0$ are known and called the *initial coefficients*. The other coefficients are given by

$$c_{k,\ell} = c_{k-1,\ell} + c_{k,\ell-1}.$$

We denote by H the maximum size of the absolute value of an initial coefficient. We denote by $s_{k,\ell}$ the size of the absolute value of $c_{k,\ell}$. For $k > 0$ and $\ell > 0$, we clearly have

$$s_{k,\ell} \leq H + k + \ell - 1. \tag{5.1}$$

Since this upper bound of $s_{k,\ell}$ is quite pessimistic, we introduce a constant $p \in [0, 1]$ such that $S_{k,\ell}$ below is expectedly a sharper upper bound of $s_{k,\ell}$

$$S_{k,\ell} = H + p(k + \ell - 1). \tag{5.2}$$

For instance if all initial coefficients are positive and have size H, we can take $p = 1/2$ and $S_{k,\ell}$ is actually the expected value of $s_{k,\ell}$. As we shall see, this parameter p has little impact on the key results. However, not using this parameter through our calculations would imply that all our other estimates would rely on quite pessimistic estimates, which would be questionable.

Recall that we are interested here in the blocking strategy. Let $B > 1$ be the block order, we assume that B divides n. Consider a square $B \times B$ block whose top left corner has coordinates (k, ℓ). We assume that all $c_{k,\ell+j}$ for $j = 0 \cdots B$ and all $c_{k+i,\ell}$ for $i = 0 \cdots B$ are known. The work $C_{B,k,\ell}$ for computing all the other coefficients of

the block is given by

$$C_{B,k,\ell} = \sum_{i=1}^{B} \sum_{j=1}^{B} S_{k+i,\ell+j}. \tag{5.3}$$

Indeed the work required for adding two numbers is in the order of the size of their sum. Then, elementary calculations yield

$$C_{B,k,\ell} = B^2(H + p(k + \ell + p)). \tag{5.4}$$

Similarly, we obtain the work $T_{B,k,\ell}$ of a triangular $B \times B$ block whose top left corner has coordinates (k, ℓ):

$$T_{B,k,\ell} = \sum_{i=1}^{B} \sum_{j=1}^{B+1-i} S_{k+i,\ell+j} = \frac{1}{6}B(B+1)(2Bp + p + 3pk + 3H + 3p\ell). \tag{5.5}$$

We are ready to compute the work $W(n)$ required for calculating all coefficients (except the initial ones) in the Pascal Triangle.

Proposition 3. *We have*

$$W(n) = \frac{1}{6}n(n+1)(3\,H + 2\,p\,n + p). \tag{5.6}$$

Proof ▷ We first observe that two square (resp. triangular) $B \times B$ blocks with top left corner (k, ℓ) and (k', ℓ') have the same work if and only if they are on the same band, that is, whenever $k + \ell = k' + \ell'$ holds. Secondly, we observe that the j-th band of square $B \times B$ blocks, for $0 \leq j \leq n/B - 2$, has $j + 1$ blocks. Thirdly, the band of triangular $B \times B$ blocks has n/B blocks. This leads to

$$W(n) = \sum_{j=0}^{n/B-2} (j+1)\, C_{B,j\,B,0} + \frac{n}{B} T_{B,(n/B-1)B,0}, \tag{5.7}$$

Elementary calculations lead to the conclusion. ◁

The formula of Proposition 3 shows that the work is cubic in n. It is also independent of B, which was naturally expected. When $p = 0$, we retrieve the quadratic case of Section 4.

5.3 Span for the blocking strategy

We are now interested in the span $S(n)$ required for calculating all coefficients (except the initial ones) by means of the blocking strategy.

Proposition 4. *We have*

$$S(n) = \frac{1}{6}B(6Hn - 3HB + 3pn^2 - pB^2 + p + 3H + 3pn) \tag{5.8}$$

PROOF ▷ The span of each band (of square or triangular $B \times B$ blocks) is equal to the work of a block on that band. Indeed, each block is computed serially. Thus, following the proof of Proposition 3, we have

$$S(n) = \sum_{j=0}^{n/B-2} C_{B,j\,B,0} + T_{B,(n/B-1)B,0}, \tag{5.9}$$

Elementary calculations lead to the conclusion. ◁

The formula of Proposition 4 shows that the span is quadratic in n and cubic in B. When $p = 0$, we have $S(n) = \frac{BH}{2}(2n - B + 1)$ and thus, in this case, the parallelism is

$$\frac{n(n+1)}{B(2n - B + 1)}, \tag{5.10}$$

which is asymptotically equal[1] to $\frac{n}{2B}$ for a fixed B.

When $p = 1$, we have

$$S(n) = \frac{B}{6}(6Hn - 3HB + 3n^2 - B^2 + 3H + 3n + 1), \tag{5.11}$$

and thus, in this case, the parallelism is

$$\frac{n(n+1)(3\,H + 2\,p\,n + p)}{B(6Hn - 3HB + 3n^2 - B^2 + 3H + 3n + 1)} \tag{5.12}$$

which is asymptotically equal $\frac{2n^3}{3Bn^2} = \frac{2n}{B}$, for a fixed B and a fixed H. Finally, when $p = 1/2$, similar calculations yields a parallelism which is asymptotically equal to $\frac{2n}{3B}$.

The above results show that taking into account the growth of the coefficients in Pascal's Triangle construction (or in Taylor shift computation) by the blocking strategy increases the parallelism by a factor which is at most 4.

[1]For the notion of *asymptotically equal*, see `http://en.wikipedia.org/wiki/Big_O_notation`.

5.4 Estimating parallelization overheads

In this section, we estimate the burdened span $S_b(n)$ incurred for calculating all coefficients (except the initial ones) by means of the blocking strategy. Recall that, in the fork-join parallelism model (thus assuming that all strands run in unit time) the burdened span is the maximum number of continuations (thus `cilk_spawn` statements) along a critical path. The instruction stream DAG of the blocking strategy consists of n/B binary tress $T_0, T_1, \ldots, T_{n/B-1}$ such that

- T_i is the instruction stream DAG of the `cilk_for` loop executing the i-th band
- each leaf of T_i is connected by an edge to the root of T_{i+1}.

Consequently, we have

$$\begin{array}{rcl} S_b(n) & = & \sum_{i=1}^{n/B} \log(i) \\ & = & \log(\prod_{i=1}^{n/B} i) \\ & = & \log(\Gamma(\frac{n}{B}+1)). \end{array} \tag{5.13}$$

Using Stirling's Formula, we deduce the following.

Proposition 5. *We have*

$$S_b(n) \in \Theta\left(\frac{n}{B}\log(\frac{n}{B})\right). \tag{5.14}$$

This result implies that the burdened parallelism (that is, the ratio work to burdened span) is sublinear. Another way to interpret this negative result is as follows. When B is replaced by its half, the (non-burdened) span is essentially multiplied by 2 while the burdened span is multiplied by a factor greater than 2. In other words, considering the (non-burdened) span only, the replacement of B by its half seems a good idea while it is a bad idea in the burdened span point of view.

5.5 Choosing the block order

We turn our attention to locality issues. More precisely, for an ideal cache of size Z and cache-line L, we ask how to choose the block order B so as to minimize cache misses.

We first determine the space requirement $R(B, k, \ell)$ for computing a square $B \times B$ block whose top left corner has coordinates (k, ℓ). As before, we assume that all $c_{k,\ell+j}$ for $j = 0 \cdots B$ and all $c_{k+i,\ell}$ for $i = 0 \cdots B$ are known. We assume that the largest coefficients in that block with be at $c_{k+B,\ell+j}$ for $j = 0 \cdots B$ and at $c_{k+i,\ell+B}$ for

$i = 0 \cdots B$. Those coefficients are actually the result of computing our block rooted at (k, ℓ). Indeed, we assume that the space used for the other coefficients of the block is recycled for storing the output coefficients. Thus we have

$$R(B, k, \ell) = \sum_{i=0}^{B-1} S_{k+i,\ell+B} + \sum_{j=0}^{B} S_{k+B,\ell+j}. \tag{5.15}$$

Then, elementary calculations yield

$$R(B, k, \ell) = 2HB + H + 2pBk + pk + 3pB^2 - pB + 2pB\ell + p\ell - p. \tag{5.16}$$

In particular, we have

$$R(B, 0, 0) = 2HB + H + 3pB^2 - pB - p. \tag{5.17}$$

Since each block is processed by one thread, and assuming that each thread has a private (Z, L)-ideal cache, we should always have

$$R(B, k, \ell) \leq Z \tag{5.18}$$

Experience shows that $R(B, k, \ell)$ should a portion α of Z. In our computations, $\alpha = 1/4$ yields the best results. Given H, p, α, Z one can solve for B the equation $R(B, 0, 0) = \alpha Z$. We obtain

$$B = \frac{p - 2H + \sqrt{13p^2 - 16Hp + 4H^2 + 12p\alpha Z}}{6p}. \tag{5.19}$$

Fixing $\alpha = 1/4$, $H = 1000$, $Z = 32Kb$, which are realistic values, and letting p be successively 0, 1/2 and 1, we obtain $B = 30.85$, $B = 31.53$, $B = 31.89$. For the α, H, Z, Figure 5.3 plots the block order B as a function of the probability p. We observe that p has a little impact on the value of B.

From now on we assume $\alpha = 1/4$. Formula (5.19) tells us how to choose the initial block order. However, due to the potential growth of the coefficients in the successive bands, we consider replacing B by its half after s steps. The number s is such that $R(B, s, 0) = Z$, that is, after s rows, we can no longer compute a square $B \times B$ block without incurring cache misses other than cold misses.

We solve the system of equations and inequalities

$$\begin{cases} R(B,0,0) = \alpha Z \\ R(B,s,0) = Z \\ B > 1, H > 1, Z > 0, s > 0, 1 > p > 0 \end{cases} \tag{5.20}$$

Using the `RealTriangularize` command of the `RegularChains` library in MAPLE we obtain the following defining expressions for B and s, as functions of H, Z, p:

$$\begin{cases} (2Bp + p)s + H - p - Z + (2H - p)B + 3pB^2 = 0 \\ 12pB^2 + (-4p + 8H)B + 4H - 4p - Z = 0 \end{cases} \tag{5.21}$$

We will take advantage of these estimates in the algorithms of the next chapters. Fixing $\alpha = 1/4$, $H = 1000$, $Z = 32Kb$, Figure 5.4 plots the row number s as a function of the probability p. We observe that p has a large impact on the value of s.

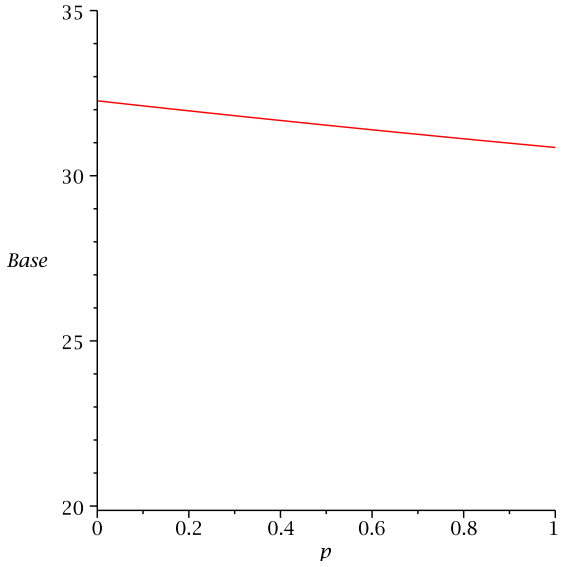

Figure 5.3: B as a function of p.

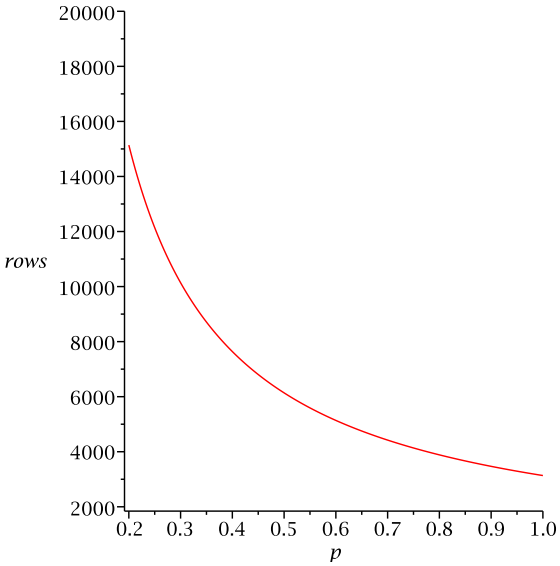

Figure 5.4: s as a function of p.

Chapter 6

Divide and Conquer Taylor shift: Dynamic approach

This chapter describes implementation techniques for Taylor shift computations using the divide and conquer scheme. Based on the study conducted in Section 5, we know that two recursive calls in the scheme are likely not to have the same work load due to the growth of the coefficients. In Chapter 3, we were using a fixed base case in the divide and conquer scheme, thus not taking into account the fact that the work load can be different for two square (or triangular) regions of the same size. Two techniques to overcome this limitation are discussed in this chapter.

A first approach, presented in Section 6.1, is to *dynamically* determine the base case, that is, the order of a square (resp. triangular) region below which the recursive division stops. A second approach, proposed in Section 6.2 is to compute the triangular regions with heavy work load as the "sum" if two triangular regions with half of the work load each. We named this second technique *partial sum*. We also consider the combination of these two techniques, that we call *combo*. Experimental results based on these techniques are reported in section 6.3 .

6.1 Divide and conquer scheme with dynamic base case

Let $p(x) \in \mathbb{Q}[x]$ be a polynomial of degree d (where $n = d + 1$) whose coefficients are stored in an array $p[0 \dots n-1]$, where $a[i]$ is the coefficient of the term of degree i. Let $q[0 \dots n-1]$ be another array of length n, where all coefficients are zero. Let α be a portion of the L1 cache, typically equal to $1/4$, for the reasons noted in Section 5.5.

Algorithm 15: `taylorShiftGeneralDynamic`$(p[0\ldots n-1], q[0\ldots n-1], \alpha)$

Input: $p[0\ldots n-1]$ is the coefficient array (dense representation) of a univariate polynomial $p(x)$ of degree d where $n = d+1$ ($a[i]$ is the coefficient of the term of degree i); $q[0\ldots n-1]$ is another array of length n, where all coefficients are initially zero; both $p[0\ldots n-1]$ and $q[0\ldots n-1]$ are overwritten; α is a portion of the L1 cache, typically equal to 1/4.

Output: Coefficient array of the polynomial $p(x+1)$ stored in the array $p[0\ldots n-1]$ such that $a[i]$ is the coefficient of the term of degree i.

```
1:  Randomly choose 10 coefficients from p;
2:  Randomly choose 10 coefficients from q;
3:  Find the largest coefficient among them;
4:  ζ = Bit size of largest coefficient;
5:  B = 1/2 − ζ/3 + ((−3+4ζ²+3αZ)^(1/2))/6
6:  if B ≤ B_min then
7:      B = B_min
8:  if n ≤ B then
9:      taylorShiftBase(p[0...n−1], q[0...n−1]);
10: else
11:     m = (n+1)/2;
12:     tableauConstruction(p[0...m−1], q[0...m−1], B);
13:     spawn taylorShiftGeneralDynamic(p[0...m−1], q[m...n−1], α);
14:     spawn taylorShiftGeneralDynamic(p[m...n−1], q[0...m−1], α);
15:     Sync
```

Algorithm 15 applied to (p, q, α) computes and stores the coefficients of $p(x+1)$ in the array $p[0\ldots n-1]$. Algorithm 15 is based on the divide and conquer scheme discussed in Chapter 3. However, and on the contrary of Algorithm 6, the base case (or threshold) B is determined dynamically.

The idea is to use Formula (5.19) from Chapter 5 in order to decide whether the current square (or triangular) region should be divided or not. When B is too small, we know from Formula (5.14) that the burdened span can be significantly larger than the span, thus reducing performances. We have determined experimentally that B should not be smaller than 25. This value should not be seen as a "Voodoo parameter". It is directly imposed by the parallelization overheads (number of cycles for `cilk_span`, etc.), see Sections 2.8.3 and 2.8.5. In our algorithms we will refer to this one as B_{min}.

In the context of Algorithm 15, we use Formula (5.19) as follows. We do not compute the maximum absolute value H of an initial coefficient, that is, the maximum

absolute value of a coefficient among those of p and q. Indeed, this would increase the work and the span of Algorithm 15 in a non-acceptable way. (Think about the recursive calls!) For this reason, we use a statistical approach: we pick randomly 10 coefficients in p and 10 coefficients in q, then use them to estimate H.

6.2 Dynamic divide and conquer scheme with partial sum

As in Chapter 5, we view the Pascal Triangle as a triangular grid, where the top left corner is the origin, with Cartesian coordinates $(0, 0)$. The coefficient in the grid with coordinates (k, ℓ) (where k is the row index and ℓ is the column index) is denoted by $P(k, \ell)$ The grid has n rows and n columns.

Computing all the coefficients $P(k, \ell)$ in a parallel fashion can be done in different ways, in particular using a divide and conquer scheme. Let us recall this scheme. Suppose that n is even and let $q = n/2$. We partition the Pascal Triangle P in three regions that we denote by C, P^+, P^- and that are defined as follows:

- for $0 \leq k, \ell \leq q - 1$ we have $C(k, \ell) = P(k, \ell)$, (which is a square region, often called a *tableau*)
- for $q \leq \ell \leq n-1$ and $k+\ell \leq n-1$, we have $P^+(k, \ell) = P(k, \ell)$, (this is top-right triangle)
- for $q \leq k \leq n - 1$ and $k + \ell \leq n - 1$, we have $P^-(k, \ell) = P(k, \ell)$. (this is down-left triangle)

We observe that computing the elements of P^+ and P^- require the knowledge of those of C. However, one can compute the coefficients of P^- into three stages:

1. Assuming that $P(q - 1, \ell) = 0$ for $0 \leq \ell \leq n - q$, compute P^- and call P_0^- the result,
2. Assuming that $P(q - 1, \ell)$ is known for $0 \leq \ell \leq n - q$ and setting $c_k = 0$ for $q \leq k \leq n - 1$, compute P^- and call P_1^- the result,
3. add P_0^- and P_1^- element-wise to deduce P^-.

We call this approach the *partial sum trick*. Figure 6.1 and Figure 6.2 shows how partial sum trick is applied to down-left triangle.

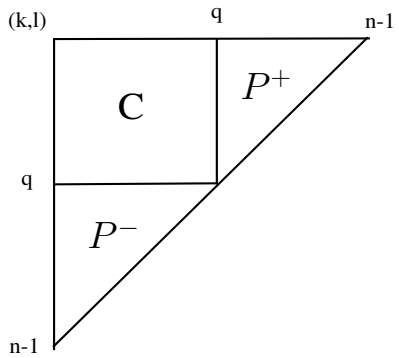

Figure 6.1: Pascal Triangle

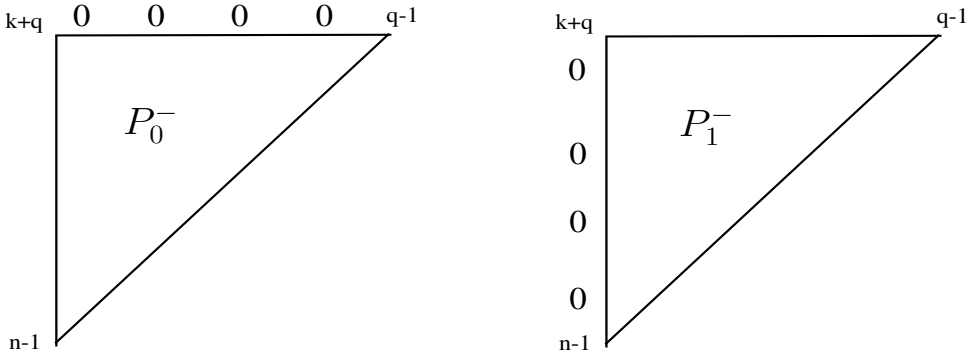

Figure 6.2: Lower triangle P^- computed in two steps P_0^- and P_1^-

Let us denote by $W_P, W_C, W_{P^-}, W_{P^+}, W_{P_0^-}, W_{P_1^-}$ the work (bit operations) for computing P, C, P^+, P^-, P_0^-, P_1^-. Similarly, let us denote by $S_P, S_C, S_{P^-}, S_{P^+}, S_{P_0^-}, S_{P_1^-}$ the span (bit operations) for computing P, C, P^+, P^-, P_0^-, P_1^-.

If the partial sum trick is not applied, then the parallelism of the divide and conquer is given by:

$$T_1/T_\infty = \frac{W_C + W_{P^-} + W_{P^+}}{S_C + \max(S_{P^+}, S_{P^-})} \tag{6.1}$$

If the partial sum trick is applied, then the parallelism becomes:

$$T_1/T'_\infty = \frac{W_C + W_{P^-} + W_{P^+}}{\max(S_C, S_{P_0^-}) + \max(S_{P^+}, S_{P_1^-})} \tag{6.2}$$

In the above, we are neglecting the work overhead and the span overhead in third stage of the partial sum trick. This is because, in practice, we only care about the *diagonal elements* of P, that is, the coefficients $P^-(k, \ell)$ for $\ell + k = n - 1$.

In order to further compare the parallelism of the two variants, we make two following genericity assumptions. We assume that we have:

- $S_{P_1^-} \geq S_{P^+}$,
- $S_C \geq S_{P_0^-}$

For instance, these assumptions hold if all c_i's are equal. Under these assumptions, we have

$$\frac{T_1/T_\infty}{T_1/T'_\infty} = \frac{\max(S_C, S_{P_0^-}) + \max(S_{P^+}, S_{P_1^-})}{S_C + \max(S_{P^+}, S_{P^-})} = \frac{S_C + S_{P_1^-}}{S_C + S_{P^-}} \tag{6.3}$$

Therefore, for the partial sum trick to improve the parallelism of the original divide and approach we need S_C to be relatively small comparing to $S_{P_1^-}$, which itself should be small comparing to S_{P^-}. The first condition is likely to happen, but the second one is not. Indeed, S_{P^-} is likely to be essentially $S_{P_1^-}$, unless the coefficients $c_{n-1}, \ldots, c_q$ are significantly larger than $c_{q-1}, \ldots, c_0$.

Algorithm 16 implements the partial sum trick.

Algorithm 16: `taylorShiftpartialSum`$(p[0 \ldots n-1], r[0 \ldots s-1], B, \alpha)$

Input: Array $p[0 \ldots n-1]$ of size n; an auxiliary array $r[0 \ldots s-1]$ of size $s = 2n$; initially $p[0 \ldots n-1]$ and $r[0 \ldots n-1]$ contain the input coefficients; $p[0 \ldots n-1]$ and $r[0 \ldots s-1]$ are overwritten during the computations; B is the base size (threshold) and α is a portion of the L1 cache, typically 1/4.

Output: Coefficient array of the polynomial $p(x+1)$ stored in the array $p[0 \ldots n-1]$ such that $a[i]$ is the coefficient of the term of degree i.

```
1:  if n ≤ B then
2:      taylorShiftBase(p[0...n−1], r[0...n−1]);
3:  else
4:      m = n/2;
5:      spawn tableauConstruction(p[0...m−1], r[0...m−1], B);
6:      spawn taylorShiftpartialSum(p[m...n−1], r[n...s−1], B, α);
7:      sync
8:      for i = n to s−1 do
9:          r[i] ← 0;
10:     spawn taylorShiftGeneralDynamic(p[0...m−1], r[m...n−1], B, α);
11:     spawn taylorShiftpartialSum(r[0...m−1], r[n...s−1], B, α);
12:     sync
13:     addVector(p[m...n−1], r[0...m−1]) ;      /*This is just a vector
        addition*/
```

Algorithm 17 combines the techniques of Algorithms 15 and 16 into a single method that we call *Combo*. The idea is to modify the scheme of Algorithm 15 as follows. When the input coefficients $p[m] \dots p[m+9]$ are sufficiently large compared to the coefficients $p[0] \dots p[9]$, the partial sum trick is applied, otherwise we follow the original scheme of Algorithm 15. This criterion is based on the estimates of Formula (6.3).

Algorithm 17: `taylorShiftCombo`$(p[0 \dots n-1], q[0 \dots n-1], \alpha)$

Input: $p[0 \dots n-1]$ is the coefficient array (dense representation) of a univariate polynomial $p(x)$ of degree d where $n = d+1$ ($a[i]$ is the coefficient of the term of degree i); $q[0 \dots n-1]$ is another array of length n, where all coefficients are initially zero; both $p[0 \dots n-1]$ and $q[0 \dots n-1]$ are overwritten; α is a portion of the L1 cache, typically equal to $1/4$.

Output: Coefficient array of the polynomial $p(x+1)$ stored in the array $p[0 \dots n-1]$ such that $a[i]$ is the coefficient of the term of degree i.

```
1:  Randomly choose 10 coefficients from p;
2:  Randomly choose 10 coefficients from q;
3:  Find the largest coefficient among them;
4:  ζ = Bit size of largest coefficient;
5:  B = 1/2 − ζ/3 + (−3+4ζ^2+3αZ)^(1/2) / 6;
6:  m = (n+1)/2);
7:  A_a = Average size of 10 coefficients p[0] ... p[9] in bits;
8:  A_b = Average size of 10 coefficients p[m] ... p[m+9] in bits;
9:  if B ≤ B_min then
10: |   B = B_min
11: if n ≤ B then
12: |   taylorShiftBase(p[0 ... n−1], q[0 ... n−1]);
13: else
14: |   if A_a + 2 * m < A_b then
15: |   |   tableauConstruction(p[0 ... m−1], q[0 ... m−1], B);
16: |   |   spawn taylorShiftCombo(p[0 ... m−1], q[m ... n−1], α);
17: |   |   spawn taylorShiftCombo(p[m ... n−1], q[0 ... m−1], α);
18: |   |   Sync
19: |   else if A_a + 2 * m ≈ A_b then
20: |   Introduce array r of size s = 2n;
21: |   r[0 ... n−1] = q[0 ... n−1];
22: |   r[n ... s−1] = 0;
23: |   taylorShiftpartialSum(p[0 ... n−1], r[0 ... s−1], B, α);
```

6.3 Experimental results

We have conducted the experiments on the implementation of our various parallelization of Taylor shift computations and VCA Algorithm on the cluster `stegosaurus.csd.uwo.ca`. This machine has one head and 13 compute nodes, called *node-0-0* to *node-0-12*. We have used *node-0-0* whose configuration is: AMD Opteron(tm) Processor 6168, L1 cache size 64KB, L2 cache size 512 KB, number of processors: 48, CPU family: 16, Model: 9, CPU MHz: 800.

We have run both static and dynamic divide and conquer schemes on different polynomial families such as BND [16], CND [16], PSnd, Chebyshev, Mignotte etc. for Taylor shift computation. *BND* and *CND* are well known experimental polynomial families introduced by Jeremy R. Johnson Werner Krandick and Anatole D. Ruslanov in their paper [16]. Let d be the degree of a polynomial in one of those families The definition of *BND* can be given as:

$$Bnd(x) = dx^n + dx^{n-1} + \cdots + dx + d$$

The definition of *CND* is:

$$Cnd(x) = x^n + d$$

Mignotte polynomial is (assuming $n >= 2$):

$$x^n - 2(5x - 1)^2$$

We define *Chebyshev* polynomial as follows. If, $T_0 = 1, T_1 = x$ then $T_n = 2T_{n-1} - T_{n-2}$.

We have introduced 3 other example polynomial families. The definition of *PSnd* can be given as:

$$PSnd(x) = 2 + 2^{(2*1)} + \cdots + 2^{2*(n-1)} + 2^{2*n}$$

Another example polynomial family *PolynomialEx1* is defined as:

$$Pex1(x) = 1 + \cdots + d * x^{n/2} + \cdots + dx^n$$

The last example polynomial family that we have introduced is *PolynomialEx2*, defined as:

$$Pex2(x) = 1 + \cdots + d * x^k + \cdots + x^n$$

where, $n/3 \leq k < n$

6.3.1 Divide and conquer: static vs dynamic

We have run both the static and dynamic divide and conquer schemes for the different polynomial families defined above. We measured their timings for both 1 processor and 48 processors, then calculated speed up. The results are shown in the Table 6.1. By static and dynamic approaches we refer to Algorithms 6 and 17, respectively.

Polynomial family	Method	n	k	Processor		Speedup
				48-Processor	1-Processor	
Bnd [16]	Static DnC	5000	5000	1.193	2.184	1.83
	Dynamic DnC	5000	5000	1.16	2.187	1.88
	Static DnC	10000	10000	5.391	16.774	3.11
	Dynamic DnC	10000	10000	5.433	16.799	3.09
	Static DnC	25000	25000	44.161	250.16	5.66
	Dynamic DnC	25000	25000	43.188	250.942	5.81
Cnd [16]	Static DnC	5000	5000	0.966	0.939	.97
	Dynamic DnC	5000	5000	0.893	0.984	1.10
	Static DnC	10000	10000	4.39	6.285	1.43
	Dynamic DnC	10000	10000	3.978	6.646	1.67
	Static DnC	25000	25000	32.523	88.158	2.71
	Dynamic DnC	25000	25000	29.356	90.631	3.08
PSnd	Static DnC	5000	NA	0.976	0.94	.96
	Dynamic DnC	5000	NA	0.903	0.994	1.10
	Static DnC	10000	NA	4.435	6.334	1.42
	Dynamic DnC	10000	NA	4.008	6.672	1.66
	Static DnC	25000	NA	31.576	88.363	2.79
	Dynamic DnC	25000	NA	30.352	91.015	2.99
Chebyshev	Static DnC	5000	NA	0.951	2.063	2.16
	Dynamic DnC	5000	NA	0.982	2.082	2.12
	Static DnC	10000	NA	4.737	15.306	3.23
	Dynamic DnC	10000	NA	4.734	15.224	3.21
Mignotte	Static DnC	5000	NA	1	0.93	.93
	Dynamic DnC	5000	NA	0.906	0.988	1.09
	Static DnC	10000	NA	4.488	6.29	1.40
	Dynamic DnC	10000	NA	3.974	6.628	1.66
PolynomialEx1	Static DnC	5000	5000	1.037	1.166	1.12
	Dynamic DnC	5000	5000	1	1.163	1.16
	Static DnC	10000	10000	4.467	8.202	1.83
	Dynamic DnC	10000	10000	4.436	8.16	1.83
	Static DnC	25000	25000	32.629	116.977	3.58
	Dynamic DnC	25000	25000	31.874	117.56	3.68
PolynomialEx2	Static DnC	5000	5000	1.004	0.932	.92
	Dynamic DnC	5000	5000	0.869	0.984	1.13
	Static DnC	10000	10000	4.586	6.292	1.37
	Dynamic DnC	10000	10000	4.106	6.642	1.61
	Static DnC	25000	25000	33.097	88.183	2.66
	Dynamic DnC	25000	25000	30.478	90.771	2.97

Table 6.1: Taylor shift computation (timings in seconds) [`Platform:stegosaurus cluster node-0-0, Static base size=50`]

From Table 6.1, we can see that, for different degree polynomials in different polynomial families, the dynamic approach is faster (in terms of running time) than the static appraoch. Moreover, it has better speed up than the static method.

To show the comparative results in a better way, we provide a plot, see Figure 6.3 which shows a compares *speedup* and *parallelism* for the static and dynamic approaches, for the input CND polynomial of degree 25,000, running on our AMD machine.

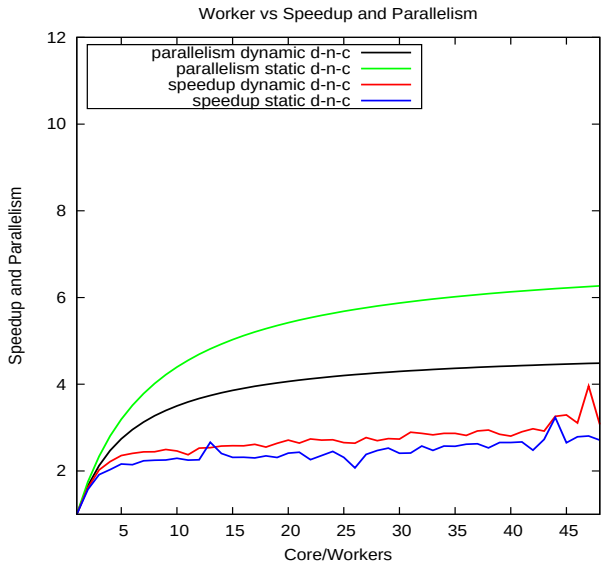

Figure 6.3: Speedup and parallelism comparison between static and dynamic divide and conquer for degree $25,000$ `Cnd` polynomial.

From Figure 6.3 it is clearly seen that dynamic approach has better speed up comparing to static method. Although the parallelism (which is a theoretic measure) seems higher for the static divide and conquer, more cache hits bring comparatively better performance to the dynamic method.

From Figure 6.4 it is clearly seen that for different number of processors *wall time* of the dynamic divide and conquer approach is better than for the one. To generate this graph, we took *trial results* generated by *Cilkview* for 1 to 48 Processors for input CND polynomial (degree 25,000) running on our AMD machine.

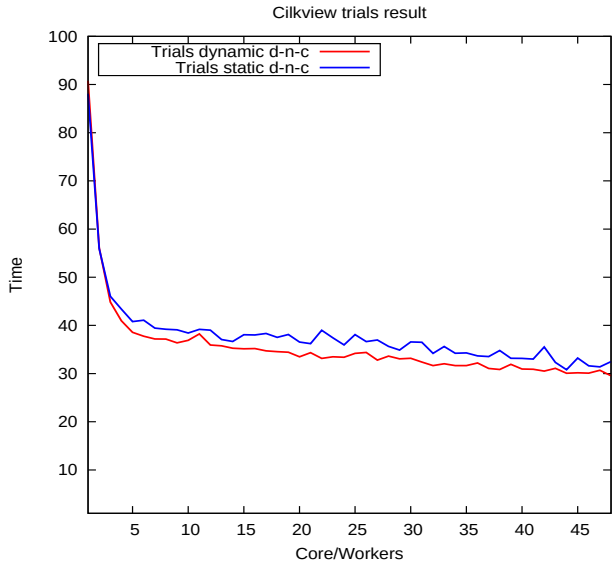

Figure 6.4: Real timing comparison between static and dynamic divide and conquer for degree $25,000$ `Cnd` polynomial.

6.3.2 Comparative results: Partial sum vs divide and conquer

We have stated in section 6.2 that there are examples where we have significantly large polynomial coefficients at the end of the Pascal Triangle. In those cases we will gain better performance if we follow the partial sum trick. To justify this, we have made a special polynomial family, (we named it *PSnd*) for which we have made a comparative study between the static divide and conquer approach, the dynamic divide and conquer approach and the divide and conquer approach using the partial sum trick.

The comparative results between partial sum, static and dynamic divide and conquer for *PSnd* polynomials of different degree are shown in Table 6.2. We have run the experiment on 1 processor and 48 processors of our AMD node.

Figure 6.5 shows comparison graph for speedup between static divide and conquer, dynamic divide and conquer and partial sum for *PSnd* polynomial of degree $25,000$. From the graph it is clearly seen that partial sum trick has better speedup for this polynomial family.

Polynomial family	Method	n	k	Processor		Speedup
				48-Processor	1-Processor	
PSnd	Static DnC	5000	5000	0.976	0.94	.96
	Dynamic DnC	5000	5000	0.903	0.994	1.10
	Partial sum	5000	5000	0.808	1.288	1.59
	Static DnC	10000	10000	4.435	6.334	1.42
	Dynamic DnC	10000	10000	4.008	6.672	1.66
	Partial Sum	10000	10000	3.731	8.487	2.27
	Static DnC	25000	25000	31.576	88.363	2.79
	Dynamic DnC	25000	25000	30.352	91.015	2.99
	Partial sum	25000	25000	28.441	113.484	3.99

Table 6.2: Taylor shift computation (timings in seconds) [`Platform:stegosaurus cluster node-0-0, Static base size=50`]

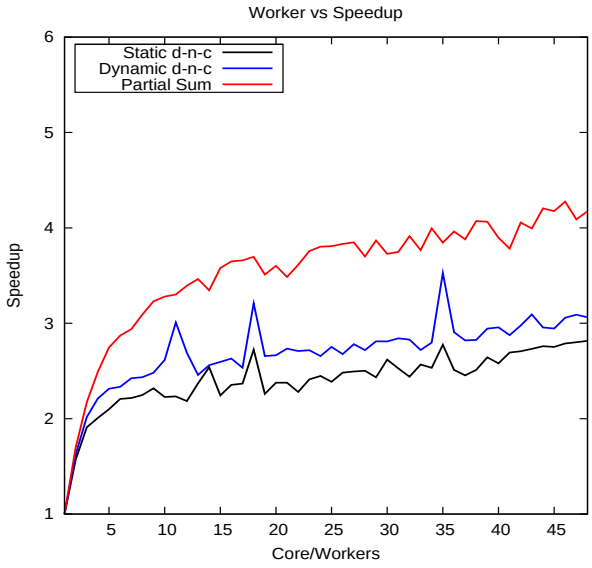

Figure 6.5: Speedup comparison between static divide and conquer, dynamic divide and conquer and Partial sum for degree $25,000$ `PSnd` polynomial.

Polynomial family	Method	n	Processor			Speedup	
			48-Proc	12-Proc	1-Proc	12-Proc	48-Proc
Chebyshev	Static DnC	400	23.411	24.846	134.821	5.42	5.76
	Dynamic DnC	400	23.584	24.977	135.035	5.40	5.73
	Static DnC	500	45.524	62.788	413.009	6.58	9.07
	Dynamic DnC	500	43.722	62.526	413.439	6.61	9.46
Mignotte	Static DnC	400	73.092	79.138	206.636	2.61	2.82
	Dynamic DnC	400	73.673	79.242	206.738	2.60	2.81

Table 6.3: Real root isolation (timing in seconds) [`Platform:stegosaurus cluster node-0-0, Static base size=50`]

Polynomial family	Method	n	Processor			Speedup	
			48-Proc	12-Proc	1-Proc	12-Proc	48-Proc
Hilbert 16	Static DnC	426	163.094	200.484	1119.02	5.58	6.86
	Dynamic DnC	426	162.13	200.068	1120.19	5.60	6.91

Table 6.4: Real root isolation Hilbert-16 (timing in seconds) [`Platform:stegosaurus cluster node-0-0, Static base size=50`]

6.3.3 Root isolation results

We have tried root isolation for well known polynomials *Chebyshev* and *Mignotte* on the same cluster node. The real root isolation results for *Chebyshev* and *Mignotte* polynomials (of different degrees) for the *static divide and conquer* and *Dynamic divide and conquer* are shown in Table 6.3.

From the above table we can see that the dynamic divide and conquer brings better speedup for isolating real roots for Chebyshev polynomial when degree is high (say, 500). One can observe from the same table that we have reached our maximum speedup when we have used 12 processors.

6.3.4 Root isolation results: Hilbert-16 polynomial family

In addition, we have used our software to isolate the real roots of a well known large polynomial called `Hilbert-16`. This polynomial has degree 426, and the bit size of its coefficients is 1900. It is available at `http://www.orcca.on.ca/~cchen/ammcs2011.txt`. Experimental results are shown in Table 6.4.

From Table 6.4 we can see that, for the *Hilbert 16* polynomial, the dynamic divide and conquer approach performs better than the static one.

Chapter 7

Blocking Taylor shift: Dynamic approach

This chapter describes implementation techniques for Taylor shift computations using the blocking scheme. In Chapter 4, our algorithms were using a block of fixed order B throughout the entire computation of the Pascal Triangle. Moreover, this order was the same for all test examples in the experiment of [6], namely 50.

Based on the results of Section 5.1 , in particular Section 5.5, we believe that

1. by virtue of Formula (5.19), the *initial* order B should be calculated from the maximum size H of the coefficients of the input polynomial and the L1 cache size Z,

2. the order B of the blocks can be reduced, say divided by 2, atter s/B bands, where s is given by Formula (5.21).

However, from Proposition 5, one should be aware that dividing the block order increases the burdened span faster than it increases the non-burdened span. Roughly speaking, this means that, parallelization overheads may grow faster than parallelization benefits.

Sections 7.1 and 7.2 describe algorithms which implement the above two techniques. Experimental results based on these techniques are reported in section 7.3 .

7.1 Dynamic granularity in blocking strategy

Repeating from chapter 4, where we have discussed about blocking method for Taylor shift which did not consider about growth of coefficients and had fixed base size for

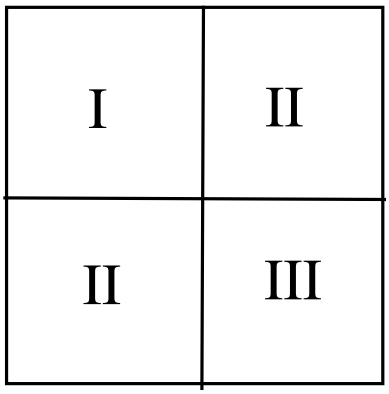

Figure 7.1: Simpler problem to show different blocking strategy

entire process. This method has several limitations, such as, this method is not cache friendly and there is room for gaining more parallelism.

We would like to consider the following issues:

1. the growth rate of coefficients.
2. blocks to be cache friendly so that it has less cache misses and
3. gain more parallelism.

Our plan is to modify static block method so that the blocks become cache aware.

For convenience to read, we rephrase our definitions that we gave in chapter 6. Let $p(x) \in \mathbb{Q}[x]$ be a polynomial of degree d (where $n = d + 1$) whose coefficients are stored in an array $a[0 \dots n-1]$, where $c[i]$ is the coefficient of the term of degree i. We denote H as coefficient size in bits. Let we denote cache as Z and α be a portion of the L1 cache, typically equal to $1/4$, for the reasons noted in Section 5.5.

From the explanation noted in Section 5.2, we observed that at the beginning of computation, if H is small then we can take many coefficients of size H inside a block without any cache miss. That makes our B bigger, the explanation can be found at Section 5.5 . During the computation H grows and size of B needs be reduced to avoid cache misses. We will go for more detailed discussion on Section 7.2. While our block size is getting smaller, we are gaining more parallelism.

To understand the idea more clearly, we brought down a simpler problem which gives the idea of dynamic changing of block size.

In this picture, we showed that a region can be divided into 4 regions, where the region I is of size 2^0, region II and III is of size 2^2. Here, by word 'size', we meant

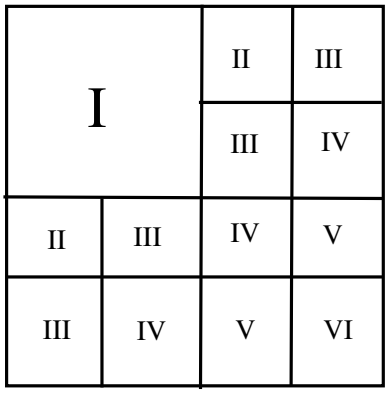

Figure 7.2: New strategy in blocking

work in that region. Assume that each of the regions have n coefficients. Region I has small coefficients. Region II and region III have bigger coefficients which makes them 4 times larger than region I.

According to the static blocking strategy, only region II works in parallel. But we can see here, we can divide region II and region III into 4 more blocks.

We can see from Figure 7.1 that 4 blocks were completed in 3 steps and we can use at most 2 workers to work parallel for region II. But, we have opportunity to introduce more workers if we follow strategy showed in Figure 7.2.

Figure 7.2 shows that region II and region III are divided into 4 more blocks. Whole problem now has 13 blocks and they are computed in 6 parallel steps, where step II can be computed with 2 workers, step III with 4 workers, step IV with 3 workers and step V with 2 workers. So, this technique gives us opportunity to introduce more workers and get more parallelism.

7.2 Cache friendly dynamic blocking

In this section we will discuss on implementation techniques for cache friendly dynamic blocking.

- At first we will compute B based on initial H and $L1$ cache size of underlying machine architecture we are working on. The function to compute B is already discussed in chapter 5 as Formula (5.19 .
- If B is bigger than n, then whole problem fits inside cache and it can be treated as just one triangle. There is no need to divide it into blocks. The entire problem is computed serially inside the cache.

- If B is smaller than n, then we will find out the number of diagonal rows we can proceed with this B before B needs to be reduced. Because, $B \times B$ ensures block of inputs can be loaded without any cache miss except cold miss and we want to know the number of rows after that we can no longer compute a square block without incurring cache misses other than clod misses. From now on we will call these diagonal rows as *Steps*. For a given B, H, $L1$ the process to get number of steps is already discussed in chapter 5 at Function 5.21 .

- Just like static blocking, there are two cases in dynamic blocking, *Regular case* and *Irregular Case*. Regular case means there will be only tableau and triangle blocks whereas for irregular case, there will be special block like trapezoid. This will only happen when n is not divisible by B.

- If we multiply B with the number of steps, that gives us the number of inputs we can proceed with block B and at which point we need to change B. If $steps * B$ is bigger than n, then we can say that entire calculation does not need to reduce B and each block will fit inside cache.

- We always know, in those steps there is a final step which will be triangle (taylor), one possible step for trapezoid (polygon) (if $n \nmid B$) and other steps should be square(tableau).

- There is a big implementation challenge for dynamic block, which is, we can not tell at beginning of dynamic block that it will have polygon blocks or not. Indeed, in static block we could tell the presence of polygons at very beginning. The reason is, the presence of polygon in program strongly depends on change of B. As an example, for input size $n = 7$ and Base size $B = 2$, we initially guess for static block that there are two steps of tableau of base 2, one step of polygon of base 2 and 1 step of triangle of base 1. But for dynamic block, if the base size becomes 1 after 2 steps of tableau, then the polygon part vanishes and instead of the polygon there will be 2 steps of tableau of base 1 and one final step of triangle. Figure 7.3 shows how the polygon parts $P_{1,1}, P_{1,1}$ and $P_{1,3}$ of sub-figure (a) change to 2 steps of tableau parts $T_{3,1}, T_{3,2}, T_{3,3}$ and $T_{4,1}, T_{4,2}, T_{4,3}, T_{4,4}, T_{4,5}, T_{4,6}$ in sub-figure(b). We take care of this issue by checking for polygon's presence at the point when we change B.

- We proceed doing tableau from beginning until the point the predicted number of steps says we should reduce our B. When we reach that point, we check if

we really need to reduce B or not. If current H still fits inside cache, then we are fine and we do not need to bother about reducing B. But if H does not fit inside cache then we reduce our B to $B/2$.

- With this reduced B we again fund out the number of steps.

  We will continue to do same process until the entire computation is done.

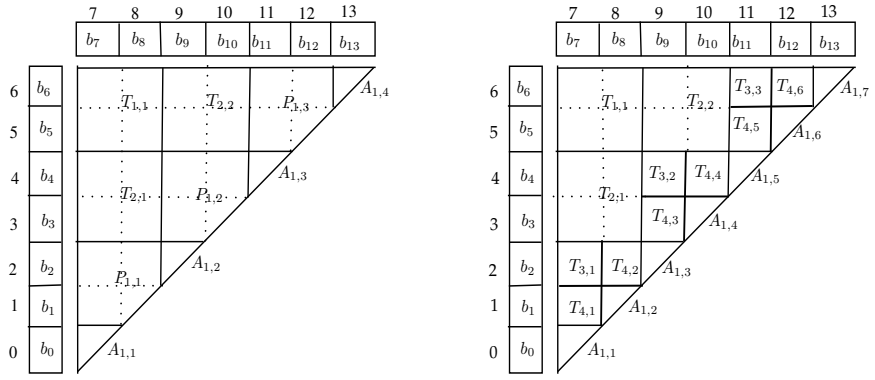

(a) When B is unchanged **(b) When B becomes B/2**

Figure 7.3: Case illustration for dynamic blocking strategy

The following algorithms show the way to implement dynamic block. Algorithm 18 and Algorithm 19 are the main controlling part. Algorithm 21 works if B remain unchanged. Whether B should be reduced or not is decided by Algorithm 22. Algorithm 23 gives the number of steps that can be continued before change on B. When B is reduced Algorithm 20 controls the computation. After tableau is completed, Algorithm 24 controls final steps such as polygons and triangles. Calculation procedure for polygon is controlled by Algorithm 25 and triangles are controlled by Algorithm 26.

Algorithm 18 applied to (a, n, α) computes and stores the coefficients of $p(x+1)$ in the array $a[0 \ldots n-1]$. Algorithm 18 is based on the blocking scheme discussed in Chapter 4. However, and on the contrary of static block algorithm, the base case (or threshold) B is determined dynamically. Algorithm 18 introduces a new array $b[0 \ldots m-1]$ of size $m = 2n$. In the context of Algorithm 18, we use Formula (5.19) and like we have discussed in Section 6.1, We do not compute the maximum absolute value H of an initial coefficient, that is, the maximum absolute value of a coefficient in b. Rather we use a statistical approach: we picking randomly some coefficients (say 100) in $b[0 \ldots n-1]$, then use them to estimate H.

We know from Formula (5.14) that, when B is too small, the burdened span can be significantly larger than the span, thus reducing performances. In Algorithm 18, we refer to this minimum value of B as B_{min}.

Before calling the dynamic block procedure, which is, basically, implemented in Algorithm 19, Algorithm 18 uses context from Section 5.5 to find out number of steps after that a square $B \times B$ block will have cache misses.

Algorithm 18: `dynamicBlock`$(a[0 \dots n-1], n, \alpha)$

Input: $a[0 \dots n-1]$ is the coefficient array (dense representation) of a univariate polynomial $p(x)$ of degree d where $n = d + 1$ ($c[i]$ is the coefficient of the term of degree i); $a[0 \dots n-1]$ is overwritten during computation and α is a portion of the L1 cache, typically equal to 1/4.

Output: Coefficient array of the polynomial $p(x+1)$ stored in the array $a[0 \dots n-1]$, such that $c[i]$ is coefficient of term of degree i.

1: $m = 2 * n$;
2: $b[0, \dots, n-1] = a[0, \dots, n-1]$;
3: $b[n, \dots, m-1] = 0$;
4: Pickup some coefficients from b and get average size of them;
5: $\zeta =$ Average coefficient size in bit;
6: $B = \frac{1}{2} - \frac{\zeta}{3} + \frac{(-3+4\zeta^2+3\alpha Z)^{\frac{1}{2}}}{6}$;
7: **if** $B < B_{\min}$ **then**
8: $\quad B = B_{\min}$
9: **if** $n <= B$ **then**
10: $\quad B = n$;
11: $\quad$ `taylorBaseBlock`$(b[0 \dots n-1], B)$;
12: $\quad a[0, \dots, n-1] = b[0, \dots, n-1]$; `/*copy results from b to a*/`
13: **else**
14: $\quad S =$ `findSteps`(B, ζ, α);
15: $\quad$ `dynamicSubBlock`$(b[0 \dots m-1], n, B, S)$;
16: **return** $a[0 \dots n-1]$;

Algorithm 19 takes all required decisions to implement a dynamic blocking scheme. With the number of steps provided to it by Algorithm 18, it proceeds computing blocks by calling Algorithm 21. Whenever it reaches to last step, it takes decision for reducing B by calling Algorithm 22. If B is decreased, computation gets a little bit tricky and to do this job Algorithm 20 is called.

Algorithm 19: `dynamicSubBlock`$(b[0 \ldots m-1], n, B, S)$

Input: $b[0 \ldots m-1]$ is the array containing coefficients of a univariate polynomial $p(x)$ of degree d ($n = d+1$), where $b[i]$ ($0 \leq i \leq n-1$), is the coefficient of the term of degree i ; B is the base size (threshold) and S is the number of steps.

Output: Coefficient array of the polynomial $p(x+1)$ stored in the array $b[0 \ldots m-1]$.

1: $\overline{B} = B$;
2: $w = 0$;
3: $e = 0$; `/*`e `is the number of blocks at each step*/`
4: $\overline{n} = n$
5: **while** ***TRUE*** **do**
6: $j = 1$
7: **if** $\overline{n} >= S * B$ **then**
8: $\overline{S} = S$
9: **else**
10: $\overline{S} = \frac{\overline{n}}{B}$
11: **if** $B = \frac{\overline{B}}{2}$ **then**
12: `newBaseHalved`$(b[0 \ldots m-1], n, B, \overline{S}, w, e)$; `/*this condition works when base size is decreased*/`
13: $\overline{B} = B$;
14: **else**
15: `baseUnchanged`$(b[0 \ldots m-1], n, B, \overline{S}, w, e)$; `/*this condition works when base size is unchanged*/`
16: $w = w + \overline{S}$; `/*`w `says how many steps are done.*/`
17: $\overline{n} = \overline{n} - (\overline{S} * B)$; `/*number of inputs that are left to do.*/`
18: **if** $\overline{S} <> S$ **then**
19: break ;
20: **else**
21: `baseDecrementDecision`$(b[0 \ldots m-1], w, B, \alpha)$; `/*this function returns new base size and new` S`*/`
22: `finalcases`$(b[0 \ldots m-1], n, w, \overline{n}, B, e, \overline{S}, \overline{B})$;

Algorithm 20: `newBaseHalved`$(b[0 \ldots m-1], n, B, \overline{S}, w, e)$

Input: $b[0 \ldots m-1]$ is the array containing input coefficients; $b[0 \ldots m-1]$ is overwritten during computation; w is the number of computed steps; B is the base size (threshold) ; number of steps $\overline{S}$ and e is the number of blocks at current step.

Output: Coefficient array of the polynomial $p(x+1)$ is overwritten on array $b[0 \ldots m-1]$ and e is the updated number of blocks.

```
1:  for j = 1 to S̄ do
2:      if j = 1 then
3:          ī = 4;
4:      else
5:          ī = 2;
6:      if j = 2 then
7:          e = e * 2;
8:      else
9:          e = e + 1;
10:     for i = 0 to e − 1 do
11:         t = n − w − (j * B) + (ī * i * B);
12:         spawn tableauBaseBlock(b[t ... t + B], B);
13:     sync
14: return b[0 ... m − 1], e ;
```

Algorithm 21: `baseUnchanged`$(b[0 \ldots m-1], n, B, \overline{S}, w, e)$

Input: $b[0 \ldots m-1]$ is the array containing input coefficients; $b[0 \ldots m-1]$ is overwritten during computation; w is the number of computed steps; B is the base size (threshold) ; number of steps $\overline{S}$ and e is the number of blocks at current step.

Output: Coefficient array of the polynomial $p(x+1)$ is overwritten on array $b[0 \ldots m-1]$ and e is the updated number of blocks.

```
1: for j = 1 to S̄ do
2:     e = e + 1;
3:     for i = 0 to e − 1 do
4:         t = n − w − (j ∗ B) + (2 ∗ i ∗ B);
5:         spawn tableauBaseBlock(b[t . . . t + B], B]);
6:     sync
7: return b[0 . . . m − 1], e;
```

When we reach base case of a block we follow the same algorithm, Algorithm 11 `tableauBaseBlock` discussed in chapter 4.

Algorithm 22: `baseDecrementDecision`$(b[0 \dots m-1], w, B, \alpha)$

Input: $b[0 \dots m-1]$ is the array containing input coefficients; w is the number of computed steps; B is the base size (threshold) ; α is a portion of the L1 cache, typically equals to 1/4.

Output: Updated B and S.

Choose 100 most recently computed coefficients and 100 input coefficients and find out the largest one.;

ζ = largest coefficient in bitsize ;

$s' =$ `findSteps`(B, ζ, α);

if $s' <= 0$ **then**

; `/*it means current block size can not contain` ζ `size coefficients without cache miss */`

$B = \frac{B}{2}$;

$S =$ `findSteps`(B, ζ, α);

else

$B = B$;

; `/*with current block size current coefficients fits inside cache */`

$S = s'$;

return B, S;

Algorithm 23: `findSteps`(B, ζ, α)

Input: B is the base size, ζ is coefficient size in bits, α is a portion of the L1 cache, typically equals to 1/4.

Output: Number of steps S that can be proceeded with current B without any cache miss.

$S := 0$;

$h = 2 * \zeta * B - \zeta + 3 * B^2 - 3 * B + 1$;

while $h < \alpha Z$ **do**

$S = S + 1$;

$h = 2 * \zeta * B - \zeta + 2 * S * B^2 - S * B + 3 * B^2 - 3 * B + 1$;

return S ;

Algorithm 24: `finalcases`$(b[0 \dots m-1], n, w, \overline{n}, B, e, \overline{S}, \overline{B})$

Input: $b[0 \dots m-1]$ is the array containing input coefficients; $b[0 \dots m-1]$ is overwritten during computation; w is the number of computed steps; $\overline{n}$ is the number of inputs that are left to compute; B is the base size (threshold) ; $\overline{S}$ is the number of steps proceeded with B and $\overline{B}$ is size of base before change.

Output: Coefficient array of the polynomial $b(x+1)$ stored in the array $b[0 \dots m-1]$.

1: $r = \overline{n}$ **mod** B;
2: **if** $\overline{S} = 1$ ***AND*** $B = \frac{\overline{B}}{2}$ **then**
3: $\quad e = e * 2$;
4: **else**
5: $\quad e = e + 1$
6: ;
7: **if** $r > 0$ **then**
; `/*when there is reminder, special case like polygons happen. */`
8: `polygonCase`$(b[0 \dots m-1], n, w, B, r, e)$;
9: **else**
; `/*when r=0 */`
10: `triangleCase`$(b[0 \dots m-1], B, e)$;

When all the square regions is computed and only the last steps like polygons or triangles are left to do, then Algorithm 24 is called. This algorithm takes decision on whether to do polygons or triangles for last steps and calls Algorithm 25 and Algorithm 26 accordingly. Algorithm 25 computes last steps if there are polygon present. Algorithm 26 works if there are only triangles at last step.

Algorithm 25: `polygonCase`$(b[0 \ldots m-1], n, w, B, r, e)$

Input: $b[0 \ldots m-1]$ is the array containing input coefficients; $b[0 \ldots m-1]$ is overwritten during computation; w is the number of computed steps; B is the base size (threshold) ; r is the size of triangles at last step and e is number of blocks at polygon step.

Output: Coefficient array of the polynomial $p(x+1)$ stored in the array $a[0 \ldots n-1]$ such that $c[i]$ is the coefficient of the term of degree i.

1: $k = B - r - 1$;
2: **if** $k > 0$ **then**
3: $\quad k = k$
4: **else**
5: $\quad k = 1$
; `/*polygon` `*/`
6: **for** $i = 0$ *to* $e - 1$ **do**
7: $\quad t = n - w + (2 * i * B)$;
8: $\quad$ **spawn** `polygonBase`$(b[t \ldots t + B], B, r, k)$;
9: **sync**
; `/*triangle` `*/`
10: **for** $i = 0$ *to* e **do**
11: $\quad$ **spawn** `taylorBaseBlock`$(b[2 * i * B \ldots 2 * i * B + r], r)$;
12: **sync**
; `/*copy triangle` `*/`
13: **for** $i = 0$ *to* e **do**
14: $\quad$ **for** $j = 0$ *to* $r - 1$ **do**
15: $\quad\quad a[j + i * B] = b[j + 2 * i * B]$;
; `/*copy polygons` `*/`
16: **for** $i = 0$ *to* e **do**
17: $\quad$ **for** $j = 0$ *to* $B - r - 1$ **do**
18: $\quad\quad a[i * B - j] = b[2 * i * B - j]$;
19: $\quad a[(i-1) * B + r] = b[2 * ((i-1) * B + r)]$;
20: **return** $a[0 \ldots n-1]$;

Algorithm 26: `triangleCase`$(b[0 \dots m-1], B, e)$

Input: $b[0 \dots m-1]$ is the array containing input coefficients; $b[0 \dots m-1]$ is overwritten during computation and e is the number of blocks for triangle step.

Output: Coefficient array of the polynomial $p(x+1)$ stored in the array $a[0 \dots n-1]$ such that $c[i]$ is the coefficient of the term of degree i.

```
1: for i = 0 to e − 1 do
2:     spawn taylorBaseBlock(b[2 ∗ i ∗ B . . . 2 ∗ i ∗ B + B], B);
3: sync
   ; /*copy from b to a                                          */
4: for i = 0 to e − 1 do
5:     for j = 0 to B − 1 do
6:         a[j + i ∗ B] = b[j + 2 ∗ i ∗ B];
7: return a[0 . . . n − 1] ;
```

When we reach base case of triangle case, we will do computations serially and follow the same algorithm discussed at Algorithm 10.

7.3 Experimental results

We have conducted the experiments on the implementation of our blocking method of Taylor shift computations and VCA Algorithm on the cluster `stegosaurus.csd.uwo.ca`. This machine has one head and 13 compute nodes, called *node-0-0* to *node-0-12*. We already have described about this machine and configuration of one of its compute node-0-0 in Section 6.3. For our experimentation we have also used another node *node-0-2* whose configuration is: Intel(R) Xeon(R) CPU X5650 with 2.67GHz processor, L1 cache size 32KB, L2 cache size 12288 KB, Number of Processors: 24, CPU family: 6, Model: 44, CPU MHz: 1600.

7.3.1 Block: static vs dynamic

We have run both static and dynamic block schemes on different polynomial families such as BND [16], CND [16], PSnd, Chebyshev, Mignotte etc. for Taylor shift computation. Definitions of these polynomial families are already specified in Chapter 6 Section 6.3. We measured their timings for both 1 processor and 48 processors and calculated speed up for both *AMD* and *Intel* machines. By static and dynamic

approaches we refer to Algorithms 13 and 18, respectively. Experimental results running on Intel machine are showed in Table 7.1.

Polynomial family	Method	n	k	Core		Speedup
				12-Proc	1-Proc	
Bnd [16]	Static block	5000	5000	0.506	1.505	2.97
	Dynamic block	5000	5000	0.493	1.505	3.05
	Static block	10000	10000	2.406	11.372	4.72
	Dynamic block	10000	10000	2.223	11.378	5.11
	Static block	25000	25000	23.551	162.654	6.90
	Dynamic block	25000	25000	21.102	162.546	7.70
Cnd [16]	Static block	5000	5000	0.401	0.628	1.56
	Dynamic block	5000	5000	0.401	0.63	1.57
	Static block	10000	10000	1.832	4.361	2.38
	Dynamic block	10000	10000	1.705	4.262	2.49
	Static block	25000	25000	14.277	60.769	4.25
	Dynamic block	25000	25000	13.493	59.743	4.42
PSnd	Static block	5000	NA	0.427	0.637	1.49
	Dynamic block	5000	NA	0.401	0.635	1.58
	Static block	10000	NA	1.798	4.381	2.43
	Dynamic block	10000	NA	1.699	4.288	2.52
	Static block	25000	NA	15.319	60.897	3.97
	Dynamic block	25000	NA	12.971	59.2	4.56
Chebyshev	Static block	5000	NA	0.403	1.392	3.45
	Dynamic block	5000	NA	0.363	1.391	3.83
	Static block	10000	NA	1.964	10.735	5.46
	Dynamic block	10000	NA	1.712	10.742	6.27
Mignotte	Static block	5000	NA	0.406	0.638	1.57
	Dynamic block	5000	NA	0.393	0.632	1.60
	Static block	10000	NA	1.902	4.335	2.27
	Dynamic block	10000	NA	1.765	4.249	2.40
PolynomialEx1	Static block	5000	5000	0.414	0.788	1.90
	Dynamic block	5000	5000	0.406	0.779	1.91
	Static block	10000	10000	1.941	5.699	2.93
	Dynamic block	10000	10000	1.865	5.571	2.98
	Static block	25000	25000	15.65	78.68	5.02
	Dynamic block	25000	25000	14.422	77.371	5.36
PolynomialEx2	Static block	5000	5000	0.384	0.627	1.63
	Dynamic block	5000	5000	0.399	0.63	1.57
	Static block	10000	10000	1.847	4.37	2.36
	Dynamic block	10000	10000	1.748	4.248	2.43
	Static block	25000	25000	14.793	61.074	4.12
	Dynamic block	25000	25000	12.788	59.821	4.67

Table 7.1: Taylor shift computation (timings in seconds) [`Platform:stegosaurus cluster node-0-2, Static block base size=25`]

Experimental results running on AMD machine are showed in Table 7.2.

From both Table 7.1 and Table 7.2, we can see that for different degree polynomials in different polynomial families, dynamic blocking method is faster than static

Polynomial family	Method	n	k	Core		Speedup
				12-Proc	1-Proc	
Bnd [16]	Static block	5000	5000	1.893	2.447	1.29
	Dynamic block	5000	5000	1.703	2.461	1.44
	Static block	10000	10000	8.269	18.819	2.27
	Dynamic block	10000	10000	8.018	18.877	2.35
	Static block	25000	25000	77.925	287.137	3.68
	Dynamic block	25000	25000	66.038	286.979	4.34
Cnd [16]	Static block	5000	5000	1.392	1.004	.72
	Dynamic block	5000	5000	1.388	1.112	.80
	Static block	10000	10000	6.996	6.976	.99
	Dynamic block	10000	10000	5.641	7.363	1.30
	Static block	25000	25000	49.911	98.978	1.98
	Dynamic block	25000	25000	48.153	99.959	2.07
PSnd	Static block	5000	NA	1.472	1.005	.68
	Dynamic block	5000	NA	1.261	1.111	.88
	Static block	10000	NA	6.643	6.994	1.05
	Dynamic block	10000	NA	6.597	7.423	1.12
	Static block	25000	NA	56.534	99.808	1.76
	Dynamic block	25000	NA	48.286	99.909	2.06
Chebyshev	Static block	5000	NA	1.332	2.266	1.70
	Dynamic block	5000	NA	1.459	2.272	1.55
	Static block	10000	NA	6.673	17.168	2.57
	Dynamic block	10000	NA	5.818	17.144	2.94
Mignotte	Static block	5000	NA	1.508	0.984	.65
	Dynamic block	5000	NA	1.474	1.094	.74
	Static block	10000	NA	6.367	6.954	1.09
	Dynamic block	10000	NA	6.868	7.355	1.07
PolynomialEx1	Static block	5000	5000	1.552	1.259	.81
	Dynamic block	5000	5000	1.445	1.325	.91
	Static block	10000	10000	7.153	9.048	1.26
	Dynamic block	10000	10000	6.028	9.386	1.55
	Static block	25000	25000	57.467	131.709	2.29
	Dynamic block	25000	25000	52.915	132.713	2.50
PolynomialEx2	Static block	5000	5000	1.483	0.988	.66
	Dynamic block	5000	5000	1.364	1.087	.79
	Static block	10000	10000	6.343	6.908	1.08
	Dynamic block	10000	10000	6.95	7.371	1.06
	Static block	25000	25000	50.193	98.866	1.96
	Dynamic block	25000	25000	47.27	99.505	2.10

Table 7.2: Taylor shift computation (timings in seconds) [`Platform:stegosaurus cluster node-0-0, Static block base size=50`]

approach (in terms of running time) . Moreover, it has better speed up than the static method.

To show the comparative results in a better way, we provide a plot, see Figure 7.4 which shows compares *speedup* and *parallelism* for the static and dynamic approaches, for input 25,000 degree BND polynomial running on our AMD machine.

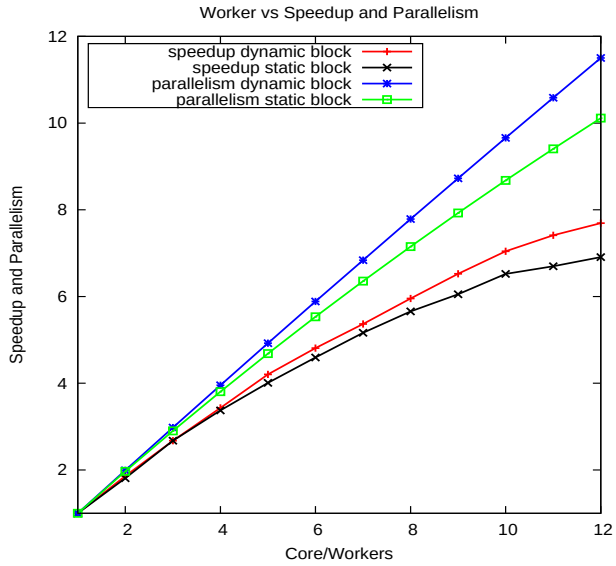

Figure 7.4: Speedup and parallelism comparison between static and dynamic blocks for degree $25,000$ `Bnd` polynomial.

Figure 7.5 shows wall timing comparison between 1-processor and 12-processor on AMD machine for different degree BND polynomial.

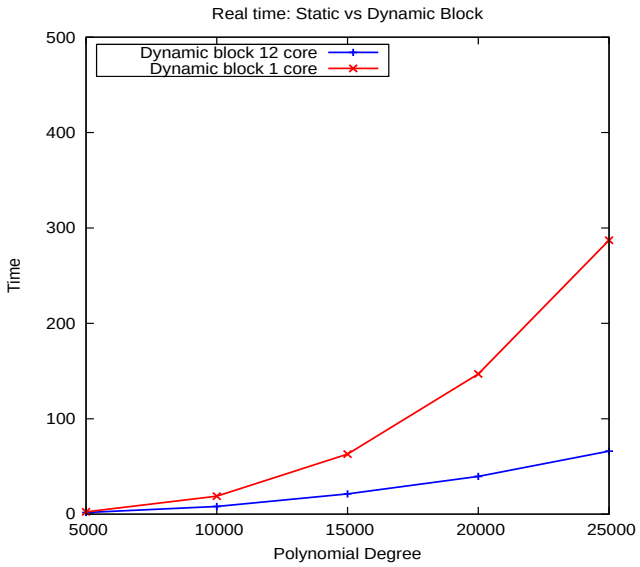

Figure 7.5: Running time for dynamic blocking for different degree `Bnd` polynomials on one core machine and 12 core machine

Polynomial family	Method	n	Core		Speedup
			12-Processor	1-Processor	
Chebyshev	Static block	400	36.413	152.304	4.18
	Dynamic block	400	35.361	152.439	4.31
	Static block	500	90.348	472.776	5.23
	Dynamic block	500	88.024	473.903	5.38
Mignotte	Static block	400	183.73	241.376	1.31
	Dynamic block	400	183.104	241.244	1.32

Table 7.3: Root isolation (timings in seconds) [`Platform:stegosaurus cluster node-0-0, Static base size=50`]

Polynomial family	Method	n	Core		Speedup
			12-Proc	1-Proc	
Hilbert 16	Static Block	426	465.227	1438.91	3.09
	Dynamic Block	426	455.388	1439.54	3.16

Table 7.4: Root isolation Hilbert-16 (timings in seconds) for Static vs Dynamic Block [`Platform:stegosaurus cluster node-0-0, Static base size=50`]

7.3.2 Root isolation results

We have tried root isolation for well known polynomials *Chebyshev* and *Mignotte* on *AMD* machine. The root isolation results for *Chebyshev* and *Mignotte* polynomials (of different degree) for static and dynamic block method are shown in table 7.3.

From above table we can see that dynamic divide and conquer brings very good speedup for isolating roots for Chebyshev polynomial.

7.3.3 Root isolation results: Hilbert-16 polynomial family

We also experimented to isolate the real roots of a well known large polynomial called `Hilbert-16`. We are repeating the specification of this polynomial from Section 6.3.4 again. It has degree 426, and the bit size of its coefficients is 1900. It is available at `http://www.orcca.on.ca/~cchen/ammcs2011.txt`. Experimental results are shown in Table 6.4.

From Table 7.4 we can see that, for the *Hilbert 16* polynomial, the dynamic block performs better than the static one.

Chapter 8

Conclusion

In this thesis, we have investigated implementation techniques for multi-threaded real root isolation of univariate polynomials targeting multi-core architectures.

We have improved previous complexity analysis (work, span, burdened span, cache) by taking into account the growth of the intermediate coefficients. This has lead to develop poly-algorithms which can adapt the granularity of their parallelism dynamically depending on the local size of the data. Experimentation illustrates the effectiveness of this approach.

Despite of these positive results, we believe that we have reached the limit of what could be done to improve multi-threaded real root isolation on multi-cores. Indeed, for this type of algorithm, as input size grows, parallelization overheads on multi-cores increase faster than parallelization benefits!

Bibliography

[1] L. A. Belady. A Study of Replacement Algorithms for Virtual Storage Computers. *IBM Systems Journal*, 5:78–101, 1966.

[2] S. Basu, R. Pollack, and M.-F. Roy. *Algorithms in real algebraic geometry*, volume 10 of *Algorithms and Computations in Mathematics*. Springer-Verlag, 2006.

[3] Robert D. Blumofe and Charles E. Leiserson. Space-efficient scheduling of multithreaded computations. In *Proceedings of the Twenty Fifth Annual ACM Symposium on Theory of Computing*, pages 362–371, San Diego, California, May 1993.

[4] Changbo Chen, James H. Davenport, John P. May, Marc Moreno Maza, Bican Xia, and Rong Xiao. Triangular decomposition of semi-algebraic systems. *CoRR*, abs/1002.4784, 2010.

[5] Changbo Chen, Marc Moreno Maza, and Yuzhen Xie. Cache complexity and multicore implementation for univariate real root isolation. *Journal of Physics: Conference Series*, 341(1):012026, 2012.

[6] Changno Chen, Marc Moreno Maza, and Yuzhen Xie. Cache complexity and multicore implementation for univariate real root isolation. *ACM Commun. Comput. Algebra*, 44:97–98, January 2011.

[7] George E. Collins and Alkiviadis G. Akritas. Polynomial real root isolation using descarte's rule of signs. In *Proceedings of the third ACM symposium on Symbolic and algebraic computation*, SYMSAC '76, pages 272–275, New York, NY, USA, 1976. ACM.

[8] Thomas Decker and Werner Krandick. On the isoefficiency of the parallel descartes method. In Götz Alefeld, Jiri Rohn, Siegfried M. Rump, and Tet-

suro Yamamoto, editors, *Symbolic Algebraic Methods and Verification Methods*, pages 55–67. Springer, 2001.

[9] Arno Eigenwillig, Vikram Sharma, and Chee K. Yap. Almost tight recursion tree bounds for the descartes method. In *Proceedings of the 2006 international symposium on Symbolic and algebraic computation*, ISSAC '06, pages 71–78, New York, NY, USA, 2006. ACM.

[10] M. Frigo, C. E. Leiserson, H. Prokop, and S. Ramachandran. Cache-oblivious Algorithms. In *Proceedings of the 40th Annual Symposium on Foundations of Computer Science*, FOCS '99, pages 285–297, New York, USA, October 1999.

[11] M. Frigo, C. E. Leiserson, and K. H. Randall. The Implementation of the Cilk-5 Multithreaded Language. In *ACM SIGPLAN*, 1998.

[12] Matteo Frigo and Volker Strumpen. The memory behavior of cache oblivious stencil computations. *The Journal of Supercomputing*, 39(2):93–112, 2007.

[13] Yuxiong He, Charles E. Leiserson, and William M. Leiserson. The cilkview scalability analyzer. In *Proceedings of the 22nd ACM symposium on Parallelism in algorithms and architectures*, SPAA '10, pages 145–156, New York, NY, USA, 2010. ACM.

[14] Hong Jia-Wei and H. T. Kung. I/O complexity: The red-blue pebble game. In *STOC '81: Proceedings of the thirteenth annual ACM symposium on Theory of computing*, pages 326–333, New York, NY, USA, 1981. ACM Press.

[15] Jeremy R. Johnson. *Algorithms for Polynomial Real root Isolation.* PhD thesis, The Ohio State University, 1991.

[16] Jeremy R. Johnson, Werner Krandick, and Anatole D. Ruslanov. Architecture-aware classical taylor shift by 1. In *ISSAC*, pages 200–207, 2005.

[17] Werner Krandick and Kurt Mehlhorn. New bounds for the descartes method. *SIGSAM Bull.*, 39:94–94, September 2005.

[18] Fabrice Rouillier and Paul Zimmermann. Efficient isolation of polynomial's real roots. *J. Comput. Appl. Math.*, 162:33–50, January 2004.

[19] Michael Sagraloff. On the complexity of real root isolation. *CoRR*, abs/1011.0344, 2010.

[20] Arnold Schönhage. *The fundamental theorem of algebra in terms of computational complexity - preliminary report.* Universität Tübingen, 1982.

[21] A. J. H. Vincent. Sur la résolution des équations numériques. *Journal de Mathématiques Pures et Appliquées*, 1:341–372, 1836.

[22] Joachim von zur Gathen and Jürgen Gerhard. Fast algorithms for taylor shifts and certain difference equations. In *Proceedings of the 1997 international symposium on Symbolic and algebraic computation*, ISSAC '97, pages 40–47, New York, NY, USA, 1997. ACM.